IDENTIFYING REGULATION OF CANT1
DURING ENDOPLASMIC RETICULUM STRESS-INDUCED CELL DEATH

by

ÖZNUR AKTAY

Submitted to the Graduate School of Engineering and Natural Sciences
in partial fulfillment of
the requirements for the degree of
Master of Science

Sabancı University
July 2018

IDENTIFYING REGULATION OF CANT1

DURING ENDOPLASMIC RETICULUM STRESS-INDUCED CELL DEATH

APPROVED BY:

Prof. Hüveyda Başağa
(thesis supervisor) .....

Prof. Batu Erman .....

Assoc. Prof. Özgür Kütük .....

DATE OF APPROVAL: 26/07/2018

ABSTRACT

IDENTIFYING REGULATION OF CANT1
DURING ENDOPLASMIC RETICULUM STRESS-INDUCED CELL DEATH

Öznur Aktay

Molecular Biology, Genetics and Bioengineering, M.Sc. Thesis, July 2018

Thesis Supervisor: Prof. Dr. Hüveyda Başağa

Keywords: CANT1, ER stress, cell death, breast cancer

Calcium-activated nucleotidase 1 (CANT1) is a member of apyrase family of enzymes which are responsible for hydrolysis of extracellular nucleoside tri-phosphate and di-phosphate to nucleoside monophosphates. The mutation in *CANT1* gene causes an autosomal recessive disorder known as Desbuquois dysplasia, revealing skeletal growth abnormalities. CANT1 is an endoplasmic reticulum (ER)-resident protein so that previous studies have suggested roles for CANT1 which are related to ER functions and mechanisms such as protein quality control or unfolded protein response. The first CANT1 expression study in cancer has emerged in prostate cancer research due to the high expression level of CANT1 in prostate tissue. In this study, we aimed to identify the regulation of CANT1 expression during ER stress-activated cell death in breast cancer cell lines MCF7, SK-BR-3, and MDA-MB-468. We induced ER stress-related cell death by Thapsigargin and investigated how the protein expression, mRNA level and subcellular localization of CANT1 change in breast cancer cell lines. Immunoblot results indicate that CANT1 protein expression was altered during ER stress while we did not observe any change in CANT1 mRNA level. Additionally, subcellular localization of CANT1 protein upon ER stress was detected by laser scanning confocal microscope and we obtained increasing colocalization of CANT1 protein with ER but not with mitochondria. Here, first time, we reported how CANT1 expression levels and its subcellular localization change in breast cancer cells upon drug-mediated ER stress-induced cell death.

ÖZET

ENDOPLAZMİK RETİKULUM STRESİ İLE İLGİLİ HÜCRE ÖLÜMÜNDE CANT1 REGÜLASYONUNUN TANIMLANMASI

Öznur Aktay

Moleküler Biyoloji, Genetik ve Biyomühendislik, Yüksek Lisans Tezi, Temmuz 2018

Tez Danışmanı: Prof. Dr. Hüveyda Başağa

Anahtar kelimeler: CANT1, ER stresi, hücre ölümü, meme kanseri

CANT1, apiraz enzim ailesine mensup, hücre dışındaki nükleozit tri- ve di-fosfatın nükleozit monofosfata hidrolizinden sorumlu bir enzimdir. CANT1 genindeki mutasyon otozomal çekinik bir hastalık olarak bilinen ve iskelet gelişiminde anormalliklere yol açan Desbuquois displazisine sebep olur. CANT1 endoplazmik retikulum (ER) yerleşik bir protein olduğu için, yapılan çalışmalar CANT1 için ER fonksiyon ve mekanizmaları ile ilgili protein kalite kontrolü ve katlanmamış protein cevabı gibi roller önermektedir. Prostat dokusunda CANT1 anlatımının yüksek seviyede olmasından dolayı, kanser konseptinde, CANT1 proteini ilk olarak prostat kanserinde araştırılmıştır. Bu çalışma ile, ER stresiyle aktifleştirilmiş hücre ölümü sırasında CANT1 anlatımının meme kanseri hücre hatlarındaki (MCF7, SK-BR-3 ve MDA-MB-468) regülasyonunu tanımlamayı hedefledik. Thapsigargin kullanarak, ER stresiyle ilgili hücre ölümünü aktifleştirdik ve meme kanseri hücre hatlarında CANT1'in protein anlatımının, mRNA seviyesinin ve hücre içi lokalizasyonunun nasıl değiştiğini araştırdık. İmmünoblot sonuçları ER stresi esnasında CANT1 proteininin anlatımının değiştiğini ortaya koyarken, mRNA seviyesinde bir değişiklik gözlemlenmedi. Bunlara ek olarak, CANT1 proteininin hücre içindeki lokalizasyonunu lazer taramalı konfokal mikroskobu ile saptadık ve CANT1 proteininin ER stresine bağlı olarak ER ile kolokalizasyonunun arttığı, fakat mitokondri ile kolokalizasyonunda herhangi bir değişim olmadığı sonucunu elde ettik. Bu çalışmada, ilk defa, ilaç kontrollü ER stresiyle uyarılmış hücre ölümünde, CANT1 anlatım seviyelerinin ve hücre içi lokalizasyonlarının nasıl değiştiğini göstermiş olduk.

to my beloved family...

ACKNOWLEDGEMENTS

I would like to express my gratitude to my thesis supervisor Prof. Hüveyda Başağa for her great support during my master's studies. Prof. Başağa is the best supervisor I could ever have. It was a milestone for me to start working in her laboratory. She encouraged and motivated me all the time. She believed me and made me feel this in every single moment that I spent in her lab. I can say that I am incredibly lucky. Her wonderful guidance will be helpful for the rest of my academic and personal life and I will always remember her advice while building my career.

I also would like to thank Assoc. Prof. Dr. Özgür Kütük for his sincere theoretical and practical support during planning and performing experiments. He gave me chance to work with exciting and promising projects, it was so great to work with his fabulous motivation. Additionally, he was always on the other side of the phone whenever I need his help. He always came up with great ideas, and he enriched my studies with his valuable comments and critics.

I would like to thank my thesis jury Prof. Batu Erman for sharing valuable comments and ideas on interesting points. Besides the things that I learned from Prof. Erman in the lectures, his guidance in confocal microscopy also was very inspirational. I could not have most of my microscopy work without his help.

I want to express my sincere thanks to former and present members of Başağa Lab for their great help; Bahriye Karakaş, Ayça Tekiner, Yelda Birinci, Can Timuçin and Sevde Nur Karataş. I am happy to have good times with such nice people in my working environment.

I am really grateful to my good fellows Işık Kantarcıoğlu, Liyne Noğay, Sanem Sarıyar and Sarah Barakat for their honest friendship and all the good memories we saved together. I also would like to express my special thanks to Özlem Yedier, Lola İkromzoda, Nazlı Kocatuğ and Furkan Güçlü for being always there to cheer me up whenever I became upset or disappointed.

There is no word to express my appreciation to my beloved parents and to my lovely sister Semanur. Their infinite and precious love always keeps me strong during ups and downs in roller coaster rides of the life.

Lastly, I would like to thank my chaperone protein Ronay for his great help, amazing support, endless patience, and unconditional love.

TABLE OF CONTENTS

LIST OF FIGURES

LIST OF TABLES

LIST OF ABBREVIATIONS

α	Alpha
β	Beta
μ	Micro
n	Nano
APS	Ammonium persulfate
BSA	Bovine serum albumin
CO_2	Carbon dioxide
DAPI	4, 6-diamidino-2-phenylindole
DMEM	Dulbecco's modified Eagle's medium
DMSO	Dimethyl sulfoxide
ECL	Enhanced chemiluminescence
EDTA	Ethylene diamine tetraacetic acid
EGTA	Ethylene glycol tetraacetic acid
GAPDH	Glyceraldehyde-3-phosphate dehydrogenase
H_2O	Water
HCl	Hydrogen chloride
HRP	Horse-radish peroxidase
KCl	Potassium chloride
kDa	Kilo Dalton
$MgCl_2$	Magnesium chloride
mRNA	Messenger RNA
MW	Molecular weight
NaCl	Sodium chloride

PAGE	Polyacrylamide gel electrophoresis
PBS	Phosphate-buffered saline
RNA	Ribonucleic acid
RT-PCR	Reverse transcription - Polymerase chain reaction
SDS	Sodium dodecyl sulfate
TEMED	Tetramethyl ethylene diamine
UDP	Uridine diphosphate
WST-1	Water Soluble Tetrazolium-1

1. INTRODUCTION

1.1. Endoplasmic Reticulum

Endoplasmic reticulum (ER) is a central organelle which consists of sacs and tubes forming a labyrinth-shaped compartment enclosed by lipid bilayer. ER system has major roles in the cell such as regulation of protein and lipid processing, protein folding and quality control, post-translational modification of proteins and calcium storage [1].

Protein processing takes place in ER lumen. Most proteins are directed to ER with a signal peptide sequence. This signal is comprised of approximately first 25 amino acids of a protein[2]. Once a signal is recognized and protein is translocated to ER lumen, protein folding machinery conducts properly folding of proteins with helper proteins called chaperones and folding enzymes. Besides being responsible for proper folding of proteins, chaperones prevent aggregation in ER to provide a cleaned-up environment for protein folding [3].

Protein modification step is required to obtain a mature protein. Co-translational and post-translational protein modification mechanisms in ER includes N-glycan addition and disulfide bond formation [4]. Oligosaccharide side chain addition to protein assists to keep its native polypeptide structure stabile, so that it prevents formation and aggregation of misfolded proteins [3]. Asparagine-linked carbohydrates are involved in quality control mechanisms of ER for unfolded and misfolded proteins. UDP-glucose:glycoprotein–glucosyltransferase (UGGT) is able to detect incomplete folding of glycoproteins and it re-glycosylates them until completing protein folding correctly [5]. Disulfide bond formation occurs when two cysteine residues covalently bind to each other and this event is monitored by protein disulfide isomerase (PDI) enzyme family in ER. As a post-translational modification, formation of disulfide bonds enhances the stability of polypeptide chain [6].

ER quality control procedure relies on checking protein folding, assembling and modification. Successfully folded mature proteins pass from ER quality control and they are

allowed to leave ER through the secretory pathway. However incompletely folded or misfolded proteins are not secreted from ER and they are directed to retention and degradation [7].

Lipid biosynthesis, another important feature of ER, takes place in the endomembrane compartment which consists of ER and Golgi apparatus. Synthesized lipids are transferred to other organelles or cell surface via secretory pathway [8].

Majority of intracellular calcium is stored in ER. Calcium homeostasis in ER is maintained by Ca^{2+} -ATPase pumps. High concentration of Ca^{2+} in ER lumen is required for proper folding [3].

1.2. ER Stress

1.2.1. Unfolded Protein Response (UPR)

Aggregation of misfolded proteins, calcium imbalance, nutrient deprivation, hypoxia, change in pH, oxidative stress and infections can disrupt ER homeostasis and they cause ER stress. The defense mechanism against ER stress conditions is called unfolded protein response (UPR) [9]. Activation of the cellular response through stress conditions is vital for deciding cell fate. UPR mediates the reestablishment of ER homeostasis by degrading misfolded proteins to clean ER lumen in order to reinforce the efficiency of protein folding machinery. In the case of ER homeostasis is not restored, stress signaling induces the expression of pro-death genes to execute cell death [10].

To activate UPR signaling, ER stress detection is required. UPR mechanism consists of chaperones and ER-resident sensors to recognize ER stress elements and to carry out downstream signaling.

1.2.1.1. Initiation of UPR signaling

ER chaperons and ER-embedded transducers of UPR signaling cooperate to sense misfolded or unfolded proteins. ER-resident chaperone BiP/Grp78 (immunoglobulin heavy chain binding protein/glucose- regulated protein 78 kDa molecular weight) is a member of heat-

shock protein (HSP) family. It sequesters nascent polypeptides while polypeptide synthesis continues. BiP chaperone has two domains, ATPase binding site at its N-terminal and substrate-binding domain at C-terminal. ATPase activity of BiP is induced when BiP binds to a polypeptide. Nucleotide exchange in BiP causes a reduction in the binding affinity of BiP to its substrate. ATP hydrolysis is required to increase the rate of BiP-polypeptide interaction affinity [11].

BiP is found to be interacted to three ER-transmembrane proteins, ATF6 (activating transcription factor 6), PERK (protein kinase RNA-like endoplasmic reticulum kinase), and IRE1 (inositol-requiring enzyme 1) and keep them inactive in unstressed environment. Initiation of UPR signaling is followed by the disassembly of BiP from ER-transmembrane sensors. Once unfolded proteins are accumulated in ER lumen, BiP dissociates from three ER stress sensors to hold accumulated proteins in the lumen. Thus, BiP unblocks the ER stress sensors and facilitates their activation of by releasing them [10].

1.2.1.2. Downstream of UPR execution

Stress response signaling is generated to determine the fate of cell that exposed to stress. The result of downstream signaling can be either restoring ER homeostasis or directing the cell to death [12]. ER-transmembrane proteins ATF6, PERK and IRE1 can operate UPR signaling (Figure 1.1) by inducing pro-survival or pro-death genes according to the reflection of ER stress. If the damage that caused by stress is too severe to maintain survival of cell, then apoptosis is activated to prevent malfunctioning. In the other scenario, if the accumulation rate of misfolded and unfolded proteins is not excessive, UPR signaling contributes to cell survival.

1.2.1.2.1 ATF6

ATF6 (activating transcription factor 6) is a type-II transmembrane protein that is positioned its C-terminal at lumen of ER and N-terminal at cytosol. There are two isoforms of ATF6 in mammals, ATF6α and ATF6β [13].

When ATF6 is activated by BiP dissociation, it translocates from ER to the Golgi to be cleaved by site-1 protease (S1P) and site-2 protease (S2P), respectively [14].

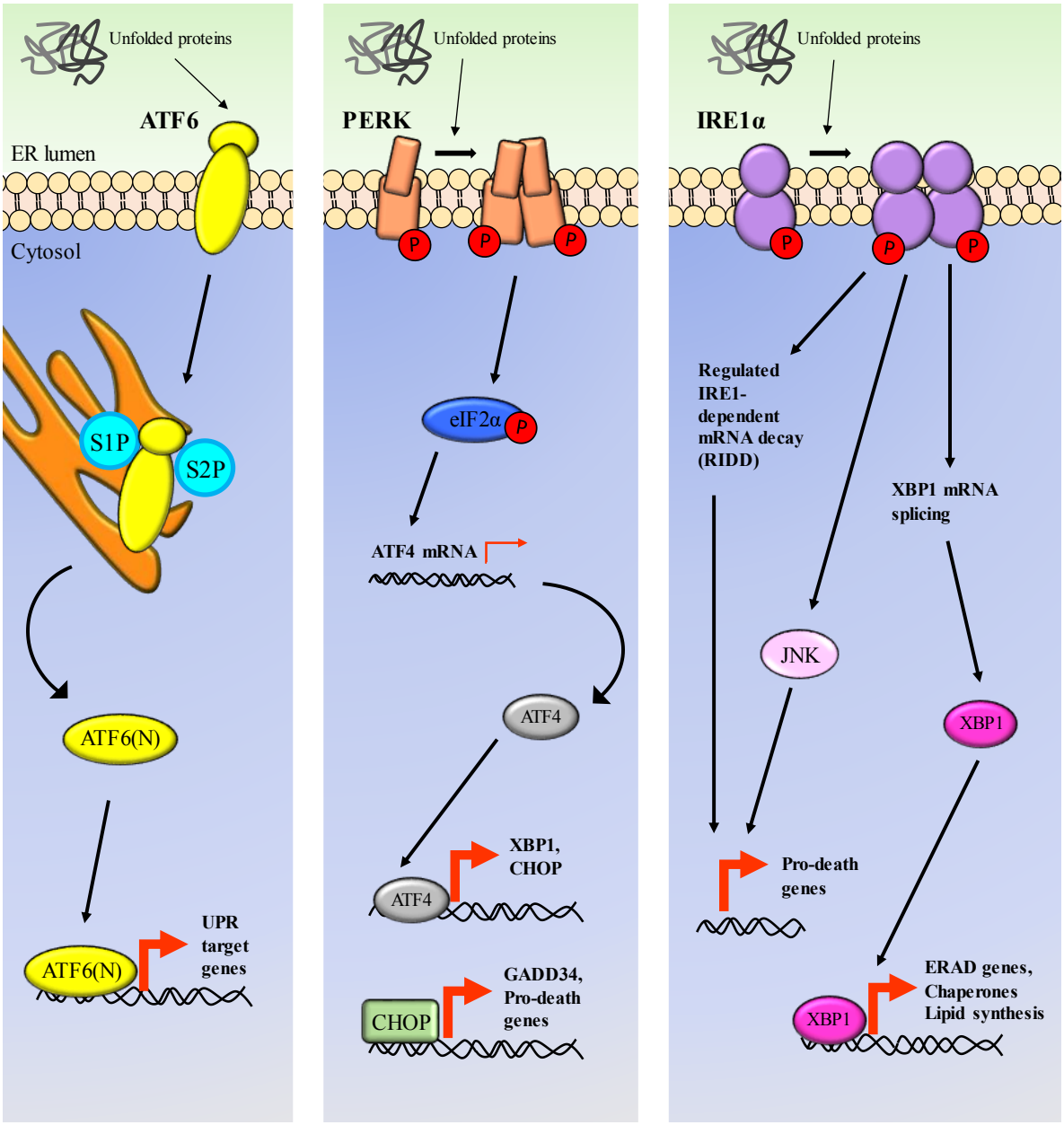

Figure 1.1. Three ER-resident proteins that execute unfolded protein response. ATF6, PERK and IRE1 are the sensors of UPR signaling. In unstressed environment, BiP has an interaction with ER transmembrane sensors. Accumulated unfolded proteins recruits BiP chaperon to ER lumen so that the sensors are released and activated. ATF6 is translocated to the Golgi to be cleaved and then ATF6(N) moves into nucleus to induce its target genes. After releasing from BiP, PERK dimerizes and auto-phosphorylates itself and the eukaryotic translational initiation factor eIF2α. Phosphorylation of eIF2α activates the expression of ATF4, which regulates its targets XBP1 and CHOP. Oligomerization and auto-phosphorylation is also observed in IRE1. Upon its activation, one branch of IRE1 signaling is involved in splicing of XBP1 mRNA. This splicing enhances XBP1's transcriptional activity that has an effect to reconstruct ER homeostasis. Alternatively, IRE1 is associated with initiation of cell death either by interacting pro-apoptotic elements of death pathway or JNK (c-Jun-N-terminal kinase) signaling [15].

Cleavage of ATF6 is processed through its N-terminus which contains bZIP (basic leucine zipper motif) transcription factor domain. This cytoplasmic domain (N-ATF6) then migrates into nucleus to activate transcription of genes that are related to ER stress regulation such as ER chaperones and ERAD (ER-associated degradation) proteins. The genes that ATF6 targets are BiP/GRP78, GRP94 (glucose-regulated protein 94), XBP1 (X-box binding protein 1), CHOP (transcription factor C/EBP homologous protein, also named GADD153), and PDI [12, 14].

1.2.1.2.2 PERK

Another UPR pathway executer is PERK (protein kinase RNA-like endoplasmic reticulum kinase) which is a type-I ER transmembrane protein. PERK is known as a serine/threonine kinase [16]. Upon disengage from BiP, PERK dimerizes and auto-phosphorylates itself to initiate and conduct stress respond signaling [12].

Active PERK phosphorylates the eukaryotic translational initiation factor eIF2α. Phosphorylation of eIF2α reduces the rate of global translation, and this reduction assists to gain ER homeostasis back in terms of preventing more aggregation by effecting the rate of protein transfer into ER. However selective translation can take place during translational blockage. ATF4 (activating transcription factor 4) mRNA translation is one example of selective translation [17]. ATF4 is a transcription factor that mainly regulates the transcription of its target genes GADD34 (growth arrest and DNA damage-induced transcript 34), XBP1 and CHOP [18]. Expression of CHOP controls the activation of pro-death genes [19, 20] while it also can inhibit the expression of anti-apoptotic protein Bcl-2 (B-cell lymphoma 2) [21].

1.2.1.2.3 IRE1

IRE1 (inositol requiring enzyme 1) is the third member of ER transmembrane sensors. It is a type-I transmembrane protein that has serine/threonine kinase domain and endoribonuclease domain. IRE1α and IRE1β are mammalian homolog forms of IRE1p which is synthesized in yeast [22].

Under stress conditions, after IRE1 dissociates from BiP, it oligomerizes and activates kinase and RNase domains by auto-phosphorylation [23]. Once it is activated, endoribonuclease domain of IRE1 cleaves its target mRNA XBP1, and causes a frameshift that generates bZIP

transcription activation of XBP1. As a transcription factor, XBP1 is responsible for expression of the genes that mediate the recovery of ER homeostasis. XBP1 enhances ER protein folding capacity by leading expression of ER chaperones and ERAD proteins [24].

Regulated IRE1-dependent mRNA decay (RIDD) is an adaptive mechanism in which ER-related mRNAs are degraded [25]. Removal of ER-related mRNAs by RIDD manages the workload of ER to allow ER to function efficiently. This case explains the role of RIDD in supporting cell survival. However, extended and continuous RIDD processing can induce pro-apoptotic genes and causes cell death [26]. IRE1 also contributes to JNK (c-Jun-N-terminal kinase) pathway-linked cell death [27].

1.2.2. Pharmacological Inducers of ER Stress

1.2.2.1. Thapsigargin

Thapsigargin (THG) is a plant-originated chemical compound that belongs to sesquiterpene lactones group [28].

The biological role of Thapsigargin is to inhibit the sarcoplasmic or endoplasmic (sarco/endoplasmic) reticulum calcium-ATPase (SERCA) family pumps which are responsible for the transfer of cytosolic Ca^{+2} ions into their storage compartment ER [29]. Inhibited SERCA activity causes Ca^{+2} leakage and, consequently, Ca^{+2} depletion in ER. Since ER Ca^{+2} homeostasis is disrupted by blocking the SERCA, it induces ER stress that resulting cell death. Interaction of Thapsigargin and SERCA is mediated by a lipophilic approach [28]. X-ray structure analysis revealed that side chains of Thapsigargin penetrate alpha-helix structures of SERCA. Upon binding covalently, the blocked pump is not able to change its conformation to transport Ca^{+2} ions actively [30].

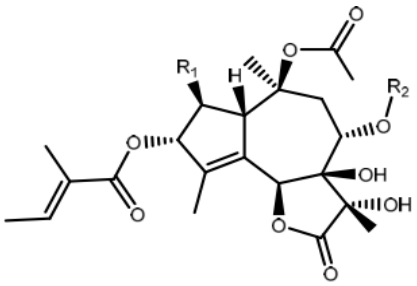

Figure 1.2. Structure of Thapsigargin (Adapted from reference [28])

SERCA in humans is encoded by three genes: *SERCA1*, *SERCA2* and *SERCA3*. Additionally, SERCA has isoforms that obtained by alternative splicing [31]. Thapsigargin can act on all isoforms of SERCA [29]. On the other hand, it is previously reported that several established Thapsigargin analogues differently but effectively inhibit the enzymatic activity of SERCA [32, 33].

Since Thapsigargin exposed cells undergo apoptotic cell death, Thapsigargin is thought to be used as a therapeutic agent that targeting certain cancer types. For this purpose, prodrugs were generated by attaching Thapsigargin to specific peptide groups. Thus, designed prodrug becomes active only in certain cancer cells due to its specific affinity [30, 34, 35].

1.2.2.2. Other chemical inducers

Various chemicals target ER function to disrupt its homeostasis through interfering different components of ER.

Tunicamycin is one of the widely used ER stress inducers. It is an antibiotic and it is produced in bacteria named *Streptomyces lysosuperificus* [36]. Tunicamycin behaves as an inhibitor of asparagine-linked glycosylation which is an important step of protein quality control mechanism in ER [37]. The other chemical agent that has an inhibitory effect on N-linked glycosylation is 2-deoxy-D-glucose (2DG) [38].

Calcium ionophores ionomycin and A-23187 causes the increase of cytosolic Ca^{+2} level by carrying luminal Ca^{+2} from ER to cytosol. Then, ER becomes Ca^{+2}-deficient and ER stress is induced [39].

Brefeldin A (BFA) prevents proteins to be transported from ER to the Golgi through the secretory pathway, and accumulation of proteins in ER causes ER stress [40].

One group of chemical ER stressors are the reducing agents β-Mercaptoethanol (2-Mercaptoethanol, BME) and Dithiothreitol (DTT) [39]. They restrict disulfide bond formation between two cysteine residues during protein folding. Finally, unfolded proteins triggers ER stress.

Other chemical agents that induce ER stress are Geldanamycin and Bortezomib. Geldanamycin inhibits the function of HSP90 (Heat shock protein 90), and the proteasome

inhibitor Bortezomib is used as an anti-tumor medication that is commercially available [39].

1.3. Mode of ER Stress in Cancer

Studies have elucidated the relation between ER stress and cancer. In cancer, to gain ER homeostasis back by the adaptive mechanism UPR is considered as maintaining a suitable environment for cell survival and growth [41]. Hypoxia, lack of nutrient, changes in pH, insufficient vascularity are stress conditions that restrict the growth of tumor cells and these stress conditions induce UPR in cancer. During tumor development, cancer cells need rapid and active cellular mechanisms to proliferate highly. Requirements for increased growth rate are advanced protein folding, modification and transportation which take place in ER. Unexpected increase in these cellular events causes ER stress, however the response to ER stress conditions has mainly a protective role for cancer cells [42, 43].

UPR sensor proteins (ATF6, PERK and IRE1), their collaborator chaperone proteins and downstream elements of UPR control tumor development through various aspects. Initiation of tumorigenesis, supporting cell growth, proliferation and survival, activation of anti-apoptotic mechanisms, regulation of metastasis and invasiveness, and establishment of angiogenesis are examples of how UPR agents involve in the management of cancer development. The high number of ER stress mechanism members in cancer progression offers a wide range of target for anti-cancer therapy.

The major ER chaperone BiP/Grp78 is overexpressed in several cancer types including breast cancer [44], pancreatic cancer [45], colorectal cancer [46], gastric cancer [47], renal cell carcinoma [48], glioblastoma [49] and ovarian cancer [50]. It is reported that BiP/Grp78 is required to mediate tumor development, cell survival and angiogenesis [51]. BiP/Grp78 also plays an important role in metastasis and drug-resistance mechanisms [47]. In colorectal cancer, expression of BiP/Grp78 is associated with response to chemotherapy [46]. In addition, the invasiveness of hepatocellular carcinoma is triggered by BiP [41].

Activation of ATF6 controls tumor progression specifically through metastasis and invasion mechanisms of cancer [52]. In the dormant state of carcinomas, transcription factor ATF6α supports tumor cell survival by activating Rheb (Ras homolog, mTORC1 binding)-mTOR

signaling [53]. One recent study revealed that high ATF6 expression was detected in atypically changing lesions of colorectal cancer [54]. Another study showed that the enhanced survival of glioblastomas was supported by an ATF6 regulated mechanism [55].

The role of PERK in cancer cell proliferation and tumor growth is mostly controlled through its downstream elements eIF2α and ATF4. PERK/ATF4 signaling sustains angiogenesis mechanism to enrich vascularization in tumor microenvironment for proliferation of tumors. ATF4 directly binds to the promoter of *VEGF* (Vascular endothelial growth factor) and activates the expression of VEGF to increase vascularity [56]. Under hypoxic stress in breast cancer cells, ATF4 involves in the regulation of autophagy to promote cell survival against apoptotic cell death [57]. The eIF2α-dependent branch of PERK activation controls autophagy induction in carcinomas [58]. It is also reported that eIF2α regulates and supports metastasis under hypoxia [59]. CHOP is one of the ATF4 target genes that is expressed upon UPR activation through PERK pathway. Upregulation of CHOP is detected in hepatocellular carcinoma, and it is also shown that CHOP promotes liver tumorigenesis [60].

The third UPR sensor protein IRE1 has also significant effect on tumorigenesis. Transcription factor XBP1, the downstream target of IRE1, is highly active in several human cancer types such as breast cancer [61], pancreatic [62] and hepatocellular carcinoma [63]. XBP1 involves in the tumorigenicity of triple-negative breast cancer through the HIF1α (Hypoxia-inducing factor 1α) pathway [64]. In one study, inactivation of XBP1 splicing in multiple myeloma was suggested as a promising therapeutic option [65]. In addition to these, it has been reported that IRE1α is able to control cell proliferation in prostate cancer by regulating Cyclin A1 level and expression of ER-associated survival elements [66]. In colon cancer, the inhibition of IRE1α affects colonic tumorigenesis negatively [67]. Targeting IRE1α-XBP1 signaling in tumors proposes therapeutic approaches against tumorigenesis [62, 68].

Other chaperone proteins that contributes to UPR mechanism are also associated to cancer mechanisms. HSP90 can interact with anti-tumorigenic element p53 and can allow cancer cells to grow and survive [69]. HSP90 isoform Grp94 is related to metastasis and the inhibition of Grp94 by small molecules provides a method to treat aggressive and metastatic cancer [70]. In multiple myeloma cells, deficient Grp94 induces apoptosis, and the same deficiency in a murine xenograft model prevents the growth of myeloma [71].

UPR elements also control the genomic instability, one of the hallmarks of cancer. It was indicated that inactivation of yeast homolog of IRE1 promotes genomic instability. Deficiency in the expression PERK is also able to trigger genomic instability in mammary carcinoma [52].

1.4. ER Stress-Mediated Cell Death

UPR is thought as a survival mechanism since it is mostly engaged to gaining ER homeostasis back to provide suitable conditions for ER to function properly. If a cell is exposed to prolonged ER stress and UPR cannot restore ER homeostasis, cell death mechanisms are activated to direct the cell to death. Apoptosis and autophagy are cell death mechanisms which are monitored by ER stress signaling.

1.4.1. Apoptosis

The word 'apoptosis' was introduced first time by Kerr, Wyllie, and Currie in 1972, to identify a distinct and conserved model of cell death which possesses different morphological changings [72]. Significant morphologies of apoptosis are membrane blebbing, cell shrinkage, nuclear fragmentation and chromatin condensation [73].

Apoptosis is also known as programmed cell death (type-I programmed cell death) so that its regulation is genetically monitored. The genes that contributing to programmed death of cells was firstly identified in the nematode *Caenorhabditis elegans*. During its developmental process, the number of cells in the nematode reduces to 959 from total of 1090 cells. This organized clearance of 131 cell is conducted by apoptosis. Brenner, Horvitz and Sulston identified the C. elegans death (ced) genes and they showed the significant role of *ced-3* and *ced-4* genes in cell death [74].

Human homologs of ced are the cysteine proteases 'caspases' that cleave their targets by proteolytic activity after only aspartate residues. First introduced mammalian caspase protein was ICE (interleukin-1L converting enzyme) called now caspase-1. Caspases have central roles in apoptosis pathway are caspase-2, -3, -6, -7, -8, -9 and -10. Other caspases such as

caspase-1, -4 and -5 participate in inflammation. Caspases are inactive zymogens and they are activated upon apoptotic stimuli [75].

Physiological cell death during development of multicellular organisms is conducted by apoptosis to support tissue and organ homeostasis. Precisely regulated machinery of apoptosis eliminates the web structure between digits in fingers and toes in human embryonic stage. Role of apoptosis in development and growth can be exemplified as forming vertebrate central nervous system and palate, and controlling amphibian metamorphosis [76]. Removal of damaged, infected, malfunctioning, unhealthy or unnecessary cells by apoptosis is advantageous and favorable for organisms in terms of preventing diseases that resulting from malfunctioning of cells.

Molecular mechanism of apoptosis relies on two main pathways: extrinsic and intrinsic pathway (Figure 1.3). Extrinsic pathway, also known as death receptor pathway is activated via death receptors on the cell surface. Death ligands TNFα (tumor necrosis factor α), TRAIL (TNF-related apoptosis-inducing ligand) and FasL bind their corresponded receptors TNFR, TRAIL-R1/DR4, TRAIL-R2/DR5 and FasR, and trigger their oligomerization. Adaptor protein FADD (Fas-associated death domain) containing death domain then recruit initiator inactive caspases, pro-caspase-8 and pro-caspase-10, and form DISC (death-inducing signaling complex) to convey downstream death signaling. Once DISC is assembled, initiator caspases (pro-caspase-8 and pro-caspase-10) are cleaved and become active via autocatalysis. Other adaptor protein TRADD (TNF receptor-associated death domain) recruits FADD and pro-caspase-8 upon TNFR stimulation. FADD and TRADD interact via their death domains and form a complex to activate pro-caspase-8. Activated caspase-8 directly cleave and activate effector caspases caspase-3, caspase-6 and caspase-7. Active effector caspases execute apoptotic death of cell. Inhibition of cell surface receptor-mediated death pathway can be processed by c-FLIP (Cellular FLICE (FADD-like IL-1β-converting enzyme)-inhibitory protein) which targets and binds to DISC through FADD to make it unable to initiate and transmit apoptotic cascade [73, 77].

Second pathway of apoptosis is intrinsic or mitochondria-dependent pathway. Initiation of intrinsic pathway is triggered by various intracellular stimuli such as hypoxia, DNA damage, growth factor deprivation, accumulation of misfolded proteins, heat shock, osmotic shock,

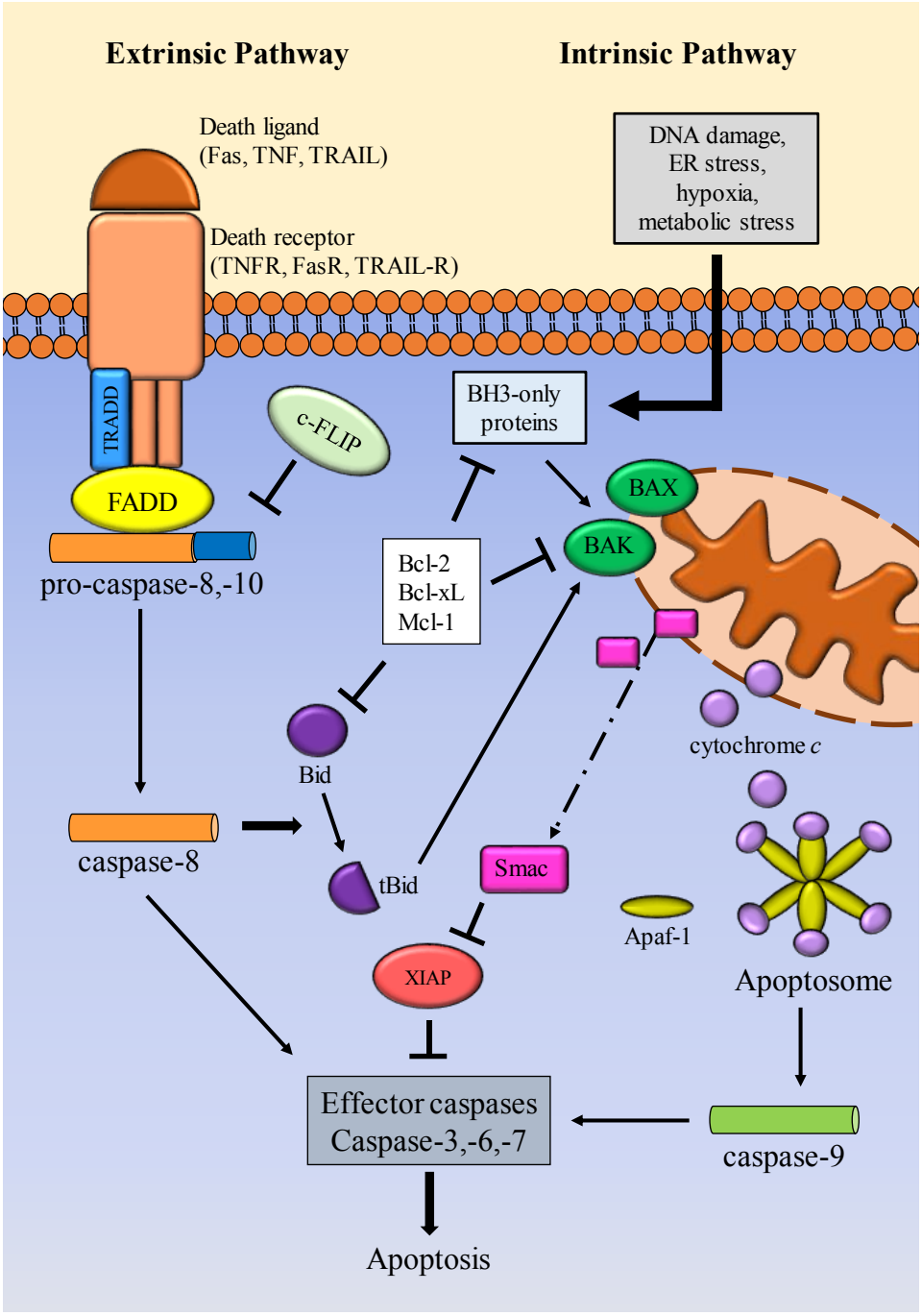

Figure 1.3. Extrinsic and intrinsic pathways of apoptotic death signaling. Cell surface death receptor activation by death ligands initiates extrinsic pathway of apoptosis. Death domain containing adaptor proteins and inactive pro-caspases are then recruited to form DISC. Following their cleavage, active initiator caspases target effector caspases to execute apoptosis. In intrinsic pathway, intracellular stimuli trigger the expression of pro-apoptotic BH3-only proteins that activates Bak/Bax proteins to initiate death signaling. Activated Bak and Bax cause MOMP, and cytochrome *c* release mediates downstream caspase activation, eventually apoptotic cell death. Anti-apoptotic Bcl-2 family proteins involve in the regulation of intrinsic pathway of apoptosis [77].

UV radiation, oxidative stress, calcium imbalance and drugs. Maintenance of mitochondrial integrity is supervised by pro-apoptotic and anti-apoptotic members of Bcl-2 family proteins. Intracellular stimuli cause oligomerization of pro-apoptotic Bcl-2 proteins Bax and Bak on the outer membrane of mitochondria and this oligomerization leads pore formation on the outer membrane, stated as mitochondrial outer membrane permeabilization (MOMP). MOMP allows leaking of proteins from intermembrane space of mitochondria into the cytosol [78]. One of these proteins is cytochrome *c* which binds to Apaf-1 (Apoptotic protease activating factor-1) to build 'apoptosome' complex. Apoptosome recruits pro-caspase-9 and activates it to initiate downstream cascade. Cleaved caspase-9 then activates effector caspases caspase-3, caspase-6 and caspase-7 to complete cell demise process. Other proteins that are released via MOMP action are Smac/DIABLO (second mitochondria-derived activator of caspase/direct IAP-binding protein with low pl), HtrA serine protease 2/Omi, AIF (apoptosis-inducing factor) and endonuclease G [78]. These released proteins are also involved in the regulation of apoptosis signaling. Smac/DIABLO and HtrA2/Omi bind IAP (inhibitors of apoptosis) proteins and prevent IAPs' inhibitory action on caspase-3, -7 and -9. AIF and endonuclease G participate in apoptosis initiation through a caspase-independent pathway. They are responsible for DNA fragmentation which is considered as an intracellular stimulus of cell death [73].

Connection between the extrinsic and intrinsic pathway of apoptosis is carried out by the Bcl-2 family protein Bid (BH3-interacting DD agonist). The route of transition is occurring from extrinsic death pathway to intrinsic mitochondrial pathway. Bid is firstly cleaved by caspase-8. Cleaved Bid is called truncated-Bid (tBid). Then, tBid is translocated to the mitochondria to interact with Bcl-2 members. As a consequence, tBid generates a mitochondria-dependent cell execution by a death receptor-mediated signaling [79].

After cells are killed by apoptosis machinery, apoptotic body structures that composed of cellular remaining take place. This apoptotic bodies are engulfed by phagocytic cells that are able to recognize "eat me" signals of dying cells. Facilitated clean-up does not cause any inflammation since spills of dying cell are enclosed by apoptotic bodies [73].

1.4.2. Bcl-2 Family Proteins and Their Role in ER Stress

The members of Bcl-2 family proteins are major controllers of apoptotic cell death. They mainly administer the balance between cell death and cell survival mechanisms through their pro-apoptotic and anti-apoptotic characteristics. Bcl-2 family proteins can be separated into three sub-class according to their apoptotic features and domains they contain in their protein structure: anti-apoptotic Bcl-2 proteins, pro-apoptotic multi-domain Bcl-2 proteins and pro-apoptotic BH3 only proteins.

Anti-apoptotic Bcl-2 proteins are Bcl-2, Bcl-xL (B-cell lymphoma extra-large, or Bcl-2-like protein 1), Bcl-w (Bcl-2-like protein 2), Mcl-1 (myeloid cell leukemia 1), A1/BFL-1 (BCL2 related protein A1), Boo/Diva/Bcl-B (Bcl-2-like protein 10) and NR-13. They are multi-domain proteins that contain Bcl-2 homology (BH) domains BH1, BH2, BH3 and BH4. Additionally, they also have a transmembrane domain (TM). They are generally located on the outer membrane of mitochondria, ER membrane or cytosol, however they translocate to MOM and ER by depending on activation [80]. Since this group of Bcl-2 family is known as anti-apoptotic or pro-survival, they are able to prevent the formation of MOMP by interacting pro-apoptotic members of Bcl-2 protein family [81].

Pro-apoptotic members of multi-domain Bcl-2 proteins are Bak (Bcl-2 homologous antagonist killer), Bax (Bcl-2 associated X protein) and Bok (Bcl-2 related ovarian killer). They have BH1, BH2 and BH3 domains in their structure. In the absence of apoptotic stimuli, subcellular location of Bax is the cytosol. Upon activation, Bax is translocated to mitochondria, and together with Bak, undergoes a conformational change. Bak and Bax then oligomerize on mitochondrial outer membrane and create pores on the membrane, resulting to permeabilization in the end [80].

Other group of pro-apoptotic proteins contains only BH3 domain so called BH3-only proteins. This group includes Bid (BH3-interacting domain death agonist), Bad (Bcl-2-associated death promoter) Bim (Bcl-2 interacting mediator of cell death), Bik (Bcl-2 Interacting Killer), Bmf (Bcl2 Modifying Factor), Hrk (Harakiri), Noxa and Puma [82].

Interaction of pro-apoptotic and anti-apoptotic proteins is mediated via shared BH3 domain, the only common domain in all Bcl-2 family proteins. The best-known interaction occurs between anti-apoptotic Bcl-2-like proteins and pro-apoptotic Bak/Bax [80]. Interaction through

BH3 domain is not restricted to only between anti-apoptotic and pro-apoptotic members of the family. Single-domain pro-apoptotic proteins also can bind Bak and Bax, multi-domain pro-apoptotic proteins. Bak and Bak can be activated by directly binding of BH3-only proteins Bim, tBid and Puma. At the same time, all BH3-only proteins can cause indirect activation of Bak/Bax by interacting anti-apoptotic members of Bcl-2 protein family [83].

Sensitizers Bad, Bmf, Bik, Hrk, Puma and Noxa selectively interact and sequester anti-apoptotic Bcl-2 proteins to prevent their pro-survival actions. For instance, Noxa is highly specific to Mcl-1 and Bad targets Bcl-2, Bcl-w and Bcl-xL. Bik and Bmf antagonize to all anti-apoptotic Bcl-2 proteins while Hrk is attracted only by Bcl-xL [81, 82].

Bax and Bak are Bcl-2 family proteins that localize on ER membrane. It is reported that they may have a role at ER stress-induced cell death since *bak-/-* and *bax-/-* double knock-out mice show resistance to ER stress-mediated apoptosis [84]. Regulation of ER calcium homeostasis by Bak and Bax shows the importance of these proteins for ER [85]. Anti-apoptotic members of Bcl-2 family tend to decrease the level of free ER calcium however Bak and Bax increase the calcium concentration [86].

Similar to Bak and Bax, *puma-/-* and *noxa-/-* cells are found to be resistant to apoptotic cell death monitored by ER stress. Puma and Noxa are indicated as highly expressed during ER stress-induced apoptosis [87]. Increase in the expression of Puma was found to be related to reduction of ER Ca^{+2} levels by Bax protein [88].

ER stress-induced apoptosis is triggered through the increased expression of BH3-only protein Bim which is controlled transcriptionally by CHOP [89].

Bcl-2 and Bcl-xL also can be positioned on the ER membrane and they show protective behaviors against ER stress [15].

It is also reported that Bcl-2 family proteins can directly affect the regulation of IRE1 [90].

1.4.3. Apoptotic Cell Death Regulation by UPR elements

Excessive ER stress leads to the initiation of signaling pathways that triggering apoptotic cell death. Three UPR sensor proteins that are mainly programmed to maintain survival of cell can also induce the activation of cell death mechanisms. Almost all components of UPR

signaling involve in the different levels of ER stress-induced apoptotic cell death pathway (Figure 1.4).

ATF6 is generally known as adaptive pro-survival [53, 55]. However, the selection of target in order to activate is dependent on the stimulus and cell type, the downstream target of ATF6 signaling can be either pro-survival or pro-death gene [10].

In the PERK-dependent branch of UPR, ATF4 is responsible from the synthesis of genes related to protein synthesis, secretion and transport. CHOP is a well-known target of transcription factor ATF4 in PERK signaling cascade. Following the induction, CHOP is able to prevent ATF4 synthesis and its own synthesis. This is an example of how PERK/ATF4/CHOP pathway contributes to cell death [86]. In one study, the level of anti-apoptotic Mcl-1 was reduced through an ATF4-dependent signaling [91]. CHOP can activate the expression of genes that controlling cell death such as DR5 (death receptor 5), also known as TRAIL-R2, in a caspase-8 dependent manner [92]. In *chop-/-* mice, decreased rate of apoptosis is observed in response to ER stress [19]. On the other hand, overexpressed CHOP causes a reduction in protein level of anti-apoptotic Bcl-2, and Bcl-2 overexpression prevents CHOP-mediated apoptotic cell death [21].

Decision of cell fate, either death or survival, by IRE1α is affected by the duration and severeness of ER stress. IRE1α promotes apoptotic cell death through activating ASK1 (apoptosis signal-regulating kinase 1) and its target JNK (c-Jun N- terminal kinase 1) by the adaptor protein TRAF2 (TNF receptor-associated factor 2). Pro-apoptotic JNK induces the activation of pro-apoptotic Bim while it inhibits anti-apoptotic Bcl-2 protein [86]. RIDD, the mRNA decay mechanism mediated by IRE1, helps alleviation of proteins in the ER to keep homeostasis in steady state. However, excess and constant RIDD processing can activates the expression of pro-death genes [26]. The transcription factor XBP1 play a significant role in cell survival [86]. Inactivation of XBP1 is associated with increasing rate of apoptosis in cancer cells [15]. Coherently, Bcl-2 protein levels was increased by depending on the overexpression of XBP1 in MCF7 cells [93].

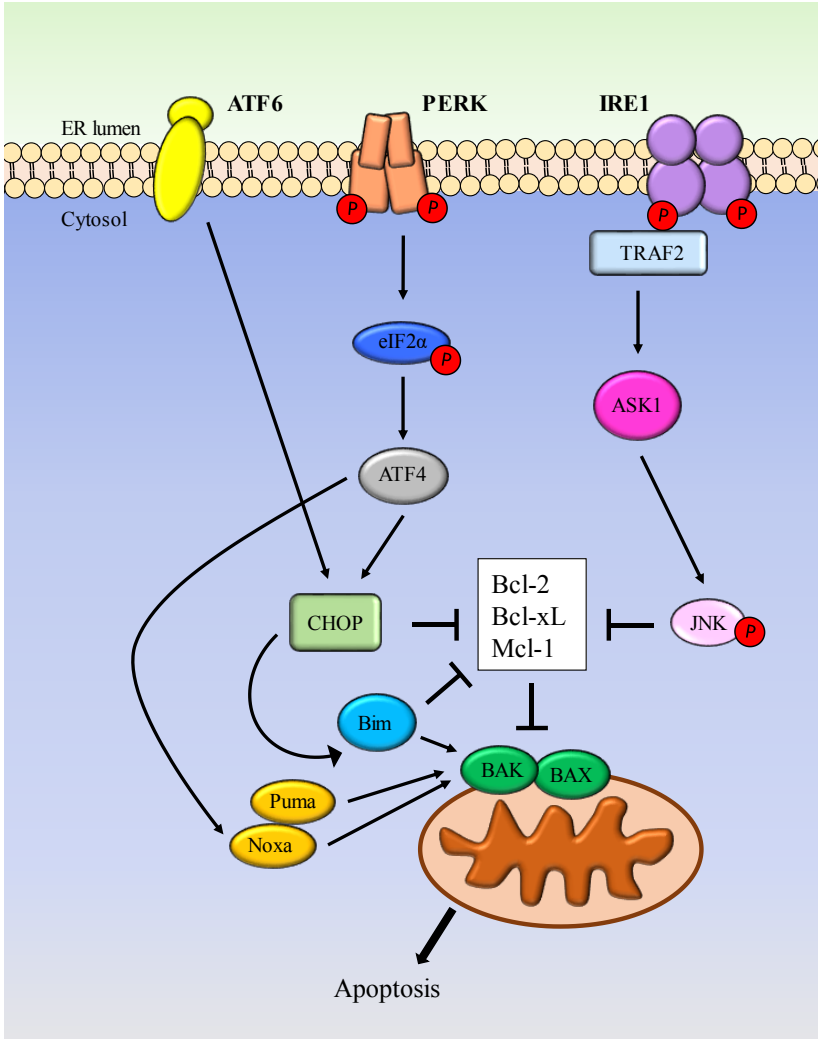

Figure 1.4. ER stress-induced cell death. Three UPR sensor proteins involve in apoptosis machinery. After its cleavage, ATF6 can activate transcription factor CHOP. PERK also induces CHOP through the phosphorylation of eIF2α, and ATF4 targets Noxa to activate Bak and Bax. CHOP induces Bim and inhibits Bcl-2 family members. Stimulated IRE1 recruits the adaptor protein TRAF2 which activates ASK1 and its downstream element JNK. JNK is able to initiate apoptosis signaling by inactivating anti-apoptotic proteins of Bcl-2 family [86].

1.4.4. Calcium Crosstalk Between ER and Mitochondria

ER is the primary storage place of calcium. To function normally, ER requires higher level of free calcium ion (500-1000μM) in ER lumen. Hence, a reduction in the level of Ca^{+2} ions can promote the activation of death signaling pathways since keeping Ca^{+2} levels stable in ER is vital for the ER homeostasis. Many chaperones of the ER work actively and efficiently with the existence of Ca^{+2} ions. Uptake of Ca^{+2} into ER is achieved by SERCA pumps, and

release of Ca^{+2} ions is processed through the inositol trisphosphate receptor (IP3R) calcium channels or ryanodine receptors [94]. Maintenance of ER calcium homeostasis is regulated by Bcl-2 family members. Studies show that Bcl-2 and Bcl-xL control ER calcium concentration by monitoring IP3R channel opening and play protective role against apoptosis [94, 95]. Another study reported that IP3R channels are also controlled by CHOP-regulated ERO1α (Endoplasmic Reticulum Oxidoreductase 1α) expression [96]. ERO1α induces calcium release from IP3R channels of ER during ER stress and triggers cell death.

Released free Ca^{+2} from ER is important for the homeostasis of mitochondria since Ca^{+2} can be up-taken by mitochondria. This calcium transfer procedure is mediated by the contact regions called mitochondria associated ER membranes (MAMs), where mitochondria and ER are in a very close-range via tethering. In MAM sites, released Ca^{+2} is accumulated in microdomains, and here take-up process is followed easily. Voltage-dependent anion channel (VDAC) play a crucial role in the sequestering of Ca^{+2} ions. Mitochondrial Ca^{+2} uniporters (MCUs) also involve in this process [97].

Calcium crosstalk between ER and mitochondria can also be ruled by Akt/PKB (Protein kinase B) [98]. Akt is able to phosphorylate IP3R channels and prevents the leakage of Ca^{+2} ions, ultimately apoptosis [99].

Prolonged ER stress causes the continuous release of calcium ions from ER lumen. Higher concentration of calcium that is taken by microdomains of mitochondria may drive apoptosis induced by the overload of calcium [88].

1.5. Calcium-Activated Nucleotidase 1 (CANT1)

Calcium-activated nucleotidase 1 (CANT1) belongs to apyrases family of enzymes that are responsible for hydrolysis of extracellular adenosine triphosphate and diphosphate (ATP, ADP) to adenosine monophosphate (AMP).

Apyrases (ATP-diphosphatase, ATP di-phosphohydrolase, adenosine diphosphatase, ADPase) family was firstly introduced as salivary apyrases in the blood-feeding arthropods. Human homologue of apyrase from arthropod bed bug *Cimex lectularius* was identified by Smith and Kirley in 2002. It was found that the enzymatic activation of the new nucleotidase

depends on calcium ion, therefore it is named human soluble calcium-activated nucleotidase 1 (hSCAN-1). Cloning, expression and characterization of SCAN-1 was performed in the same study [100].

Although apyrases are defined as ATP and ADP hydrolyzing enzymes, the preferential order of SCAN-1 substrates are indicated as UDP, GDP, UTP, GTP, ADP and ATP, respectively [100]. Addition to that, hSCAN-1 is not able to digest nucleoside monophosphates.

Bacterial expression of hSCAN-1 was performed and fully functional enzyme was obtained [101]. Refolding and constructing hSCAN-1 in bacteria did not affect enzymatic activity and this study showed that post-translational modifications are not required for the nucleotidase to function properly, since bacterial expression system does not process the post-translational modifications. In order to identify essential residues for the nucleotidase activity and enzymatic specificity of hSCAN-1, mutations were generated by site-directed mutagenesis method [102].

hSCAN-1/CANT1 is encoded by human *CANT1* gene situating at the q arm of chromosome 17. Protein product of this gene has a molecular mass of 34-37 kDa according to western blot and size-exclusion chromatography [100]. Secreted form of the enzyme exists, and the subcellular distribution of rat homologue of CANT1 was displayed on ER and ER-Golgi transition sites, since RXR ER retention motif leads to holding the Ca^{+2} nucleotidase on the ER [103].

Multiple tissue expression analysis revealed the highest mRNA levels in prostate, small intestine, testis and placenta. Lower level of mRNA was found in lung, stomach, spleen and thymus [100].

Mutation in *CANT1* gene causes Desbuquois dysplasia which is an autosomal recessive disorder causing growth retardation includes skeletal disfunctions such as joint dislocations, hand and femur abnormalities [104, 105]. In addition to the type I and type II variants of the disease, Kim variant of Desbuquois dysplasia was also defined with the additional hand bone abnormalities [106]. The role of CANT1 mutation in this disorder is unclear however one study suggests that CANT1 in Desbuquois dysplasia might involve in proteoglycan metabolism [107]. It is also speculated that the detected accumulation of inclusion bodies in ER in Desbuquois dysplasia patients might be associated with improper protein folding and accumulation of

misfolded proteins [105]. Furthermore, one recent study showed that mutations in CANT1 also cause multiple epiphyseal dysplasia (MED) which possesses clinically different characteristics from all defined types of Desbuquois dysplasia [108].

Hermans *et al*. reported that the expression of CANT1 is regulated by androgen in prostate cancer [109]. Androgen-regulated CANT1 expression pattern was also elaborated in different phases of prostate carcinogenesis in a comprehensive manner [110].

One study identifying CANT1 as a target of calcium-dependent transcriptional repressor DREAM (Downstream regulatory element antagonist modulator) proposes that CANT1 may have a role in protein synthesis and degradation, since CANT1 downregulation is associated with increasing rate of protein degradation [111].

Additionally, APY-1, the *Caenorhabditis elegans* homologue of CANT1, involves in UPR signaling in the nematode since the expression of *apy-1* is up-regulated upon ER stress signaling [112].

2. AIM OF THE STUDY

In the literature, ER-related roles and functions have been suggested for CANT1 since CANT1 is an ER-resident protein. CANT1 expression was studied in prostate cancer cells previously, regarding its high level of expression in prostate tissue. However, we did not come across any study showing the regulation of CANT1 expression in breast cancer cells. Thus, in this study, we aimed to identify how CANT1 expression is regulated in breast cancer cell lines through ER stress-induced cell death. Thapsigargin was given to MCF7, SK-BR-3 and MDA-MB-468 cells to generate ER stress by disrupting calcium homeostasis. Following that, we hypothesized the expression of calcium-activated protein CANT1 is effected in terms of protein and mRNA level when ER becomes Ca^{+2} deficient. We also wanted to learn if ER stress has an impact on alteration of the localization of ER-resident protein CANT1, or not. With other words, we thought that CANT1 localization can be affected in the lack of calcium in ER since Ca^{+2} is the cofactor for CANT1 activation. Therefore, we focused on the colocalization of CANT1 with ER and mitochondria by considering calcium crosstalk between ER and mitochondria.

By depending on our knowledge so far, this study is the first research which investigates the regulation of CANT1 expression in breast cancer cells that undergoing ER stress-induced cell death.

3. MATERIALS & METHODS

3.1. Materials

3.1.1. Chemicals

All chemicals used in this thesis are listed in Appendix A.

3.1.2. Equipment

Equipment used in this thesis are listed in Appendix B.

3.1.3. Solutions and Buffers

All solutions and buffers used in this study are listed in Appendix C.

3.1.4. Growth Media

DMEM/F12 (1:1): DMEM/F12 growth medium was supplemented with 10% fetal bovine serum (FBS) and 1% Pen/Strep (100 Units/ml Penicillin and 100 μg/ml Streptomycin) antibiotics.

Freezing Medium: Freezing medium containing 20% DMSO and 80% FBS was used to freeze all mammalian cell lines.

3.1.5. Molecular Biology Kits and Reagents

Molecular biology kits and reagents that are used in experiments in this thesis are listed in Appendix D.

3.1.6. Antibodies

Antibodies used in this thesis are listed in Appendix E.

3.1.7. Mammalian Cell Lines

ATCC Breast Cancer Cell Panel (30-4500K™) (Appendix F) and PC3 cells (ATCC® CRL-1435™) were used to screen the expression level of CANT1 protein endogenously. MCF7 (ATCC® HTB-22™), SK-BR-3 ([SKBR3] ATCC® HTB-30™) and MDA-MB-468 (ATCC® HTB-132™) breast cancer cell lines were used in the other experiments conducted in this thesis.

3.1.8. Protein Molecular Weight Marker

Protein molecular weight marker used in this thesis is listed in Appendix G.

3.1.9. Software and Programs

All software and computer-based programs that are used in this thesis are given in Table 3.1.

SOFTWARE, PROGRAM NAME	COMPANY	PURPOSE OF USE
CoLocalizer Pro 3.0.2	CoLocalization Research Software	Colocalization analysis of confocal images
GraphPad Prism 5	GraphPad Software	Design of graphics
ImageJ 1.51w	National Institutes of Health (NIH)	Densiometric analysis of immunoblot results
ZEN Blue edition 2.3	Carl Zeiss Microscopy	Post-processing of confocal images
RStudio Version 1.1.442	RStudio, Inc.	Statistical data analysis

Table 3.1. List of software and computer-based programs.

3.2. Methods

3.2.1. Mammalian Cell Culture

3.2.1.1. Maintenance of cell lines

MCF7, SK-BR-3 and MDA-MB-468 cells were grown in DMEM/F12 (1:1) complete medium and cells were incubated at 37°C with 5% CO_2. The subculturing of cells was done when they reached their confluency. Subculturing process was performed by washing the cells with 1X sterile PBS and detaching cells with proper amount of Trypsin-EDTA. By depending on experimental purpose, cells were seeded in new sterile 6-well, 12-well, 96-well or 100 mm cell culture plates.

3.2.1.2. Cryopreservation of the cells

Mammalian cells were frozen with freezing medium and kept in liquid nitrogen for further use. Cells were washed with 1X sterile PBS and trypsinized for harvesting. After cell counting, 3-5x10^6 cells were centrifuged at 300 g for 5 minutes. Then, cell pellet was resuspended with 1 ml freezing medium containing FBS and DMSO and transferred into cryovial. Cryovials were kept in a freezing container and the container was stored in a -80°C freezer to allow the temperature decrease gradually. Next day, cryovials were transferred into liquid nitrogen for long term storage.

3.2.1.3. Thawing frozen mammalian cells

Quick-thaw method was followed to thaw the cells from liquid nitrogen store. Cells were thawed in a 37°C water bath and immediately transferred into 15 ml centrifuge tube containing 9 ml of growth medium. For the removal of DMSO, centrifugation was done at 300 g for 5 minutes. Cell pellet was resuspended with growth medium and transferred into sterile cell culture plate and incubated at 37°C with 5% CO_2.

3.2.2. Treatments

Thapsigargin (THG, MW: 650.76 g/mol) was dissolved in DMSO and kept in -20°C. Dose-dependent (10nM, 100nM and 1μM) or time-dependent (4h, 8h, 16h, 24h and 48h) THG treatments were performed on MCF7, SK-BR-3 and MDA-MB-468 cells.

3.2.3. Cell Viability Assay

To detect the viabilities of cells that were exposed to THG, Cell Proliferation Reagent WST-1 Assay (Roche) manufacturer's protocol was followed. Briefly, MCF7, SK-BR-3 and MDA-MB-468 cells were seeded into 96-well plate and treated with THG as time- and dose-dependent. Then, 10 μl WST-1 reagent per well was added to cells and cells were incubated at 37°C for 4 hours. Absorbance was measured at 450nm wavelength by a microplate reader. Obtained absorbance results were demonstrated as percentage of cell viability. The absorbance of control condition was set to 100%.

3.2.4. Western Blotting

3.2.4.1. Cell harvest, cell lysis and protein isolation

Growth medium was aspirated, and cells were washed with 1X PBS. Then 1 ml of 1X PBS added to plate, and cells were collected by cell scraper and transferred into 1.5 ml centrifuge tube. Cells were span down at 300 g for 5 minutes and supernatant was removed. Cell pellet was dissolved with 1% Chaps buffer containing 5mM $MgCl_2$, 137mM KCl, 1mM EDTA, 1mM EGTA, 20mM Tris-HCl and 1% Chaps. Resuspended cells was incubated on ice for 30 minutes. Then, the lysate was centrifuged at 4°C and 13200 rpm for 10 minutes. Isolated proteins were stored at -20°C.

3.2.4.2. Measurement of protein concentration

Quick Start Bradford Assay was followed to measure the total protein concentration after isolation. Briefly, protein samples were diluted as 1:5 with double-distilled water and added into 96-well plate, and then 250 μl of Bradford solution was added per well. After 10 minutes incubation in dark, plate was read at 595nm wavelength in a microplate reader. Measured

absorbance results were used to determine protein concentrations with protein standard curve that was generated from absorbance measurement of BSA protein standards.

3.2.4.3. Preparation of SDS gel

12% SDS gel was prepared as indicated amounts in Table 3.2.

12% SDS PAGE Gel	for 1 gel (5 ml)
Acrylamide/Bis (30%)	2 ml
ddH_2O	1.75 ml
Tris-HCl-SDS, pH:8.8	1.25 ml
APS	17 µl
TEMED	3.5 µl

Table 3.2. Solutions for preparing 12% separating gel.

Spacer plate and short plate were placed in casting frame. Separating gel was poured between glass plates and isopropanol was added on top. After the gel was completely polymerized, isopropanol was removed, and gel was washed with ddH_2O several times. Then, stacking gel (Table 3.3) was poured and comb was placed.

Stacking Gel	for 1 gel
Acrylamide/Bis (30%)	325 µl
ddH_2O	1525 µl
Tris-HCl-SDS, pH:6.8	625 µl
APS	12.5 µl
TEMED	2.5 µl

Table 3.3. Solutions for stacking gel.

3.2.4.4. Sample preparation for loading

According to measured concentrations and determined loading amounts (µg), protein samples were mixed with appropriate volumes of loading buffer (4% SDS, 20% glycerol, 10% 2-mercaptoethanol, 0.004% bromophenol blue, 0.125 M Tris/HCl pH:6.8). Then, they were boiled at 95°C for 5 minutes and shortly span down before loading to gel.

3.2.4.5. Running SDS-PAGE

After gel cassette system was assembled for run, prepared samples were loaded into the gel. 1X running buffer was poured between the gel cassette system and into tank. SDS-PAGE was run at a constant voltage 100V.

3.2.4.6. Blotting (Wet transfer)

Proteins were blotted onto the membrane after the run was completed. Basically, two transfer sponges and two filter papers were submerged in freshly prepared 1X Transfer buffer. Polyvinylidene difluoride (PVDF) membrane was activated with 100% methanol and the transfer system was assembled. The closed cassette and ice block were then placed in the transfer tank and the tank was filled with 1X Transfer buffer. Blotting conditions was set as 100V, 260mA and 60 minutes.

3.2.4.7. Membrane blocking and antibody incubations

Blocking of the membrane was done with 5% milk in PBS-T solution, at the room temperature on a shaker for 1 hour. Then, primary antibody incubation was carried out as adding diluted antibody (1 µg/µl) into primary antibody incubation solution. Incubation was proceeded overnight at 4°C. After primary antibody incubation, membrane was washed with PBS-T solution for 10 minutes. This wash step was repeated for three times. HRP-linked secondary antibody was prepared in 5% milk solution and incubation was done in the room temperature for 1 hour.

3.2.4.8. ECL incubation and imaging

After required washes with PBS-T solution, the membrane was incubated with commercial ECL (Luminata Crescendo Western HRP Substrate, Millipore, USA) for 1 minute and bands were visualized by LAS4000 imaging system (Fujifilm, Japan).

3.2.4.9. Densiometric analysis

Densiometric analysis of western blotting results was performed in ImageJ software by normalizing CANT1 protein band densities to corresponded Actin band densities. Analysis results were expressed as percentages.

3.2.5. RNA Isolation

Cells were washed with sterile 1X PBS and were detached by trypsinization. Collected cells were centrifuged at 300 g for 5 minutes. Then, total RNA was isolated by RNeasy RNA isolation kit (Qiagen, Germany) according to manufacturer's protocol. Total RNA concentrations and A_{260}/A_{280} ratio were measured and determined spectrophotometrically by NanoDrop 2000 (Thermo Fisher).

3.2.6. Real time RT-PCR

Quantification of RNA was conducted by real-time one-step RT-PCR SYBR Green I detection. QuantiTect SYBR Green RT-PCR Kit (Qiagen, Germany) was used to quantify *CANT1* gene expression. Experimental setup was followed according to manufacturer's protocol. Briefly, master mixes were prepared for CANT1 and GAPDH primers (Table 3.4) that were purchased as QuantiTect Primer Assays (Qiagen) and 200 ng template RNA were used per reaction (Table 3.5).

PRIMER NAME	CATALOG NUMBER	COMPANY
CANT1	QT00003444	QIAGEN
GAPDH	QT00079247	QIAGEN

Table 3.4. Primers used in real-time one-step RT-PCR analysis.

Component	Volume/reaction	Final Concentration
2X SYBR Green Master mix	5 µl	1X
10X Primer	1 µl	1X
RT Mix	0.1 µl	-
Template RNA	Variable	200 ng/µl
RNase-free water	Variable	-
Total reaction volume	**10 µl**	

Table 3.5. Reaction setup for real-time one-step RT-PCR.

After reaction mixture was prepared, PCR was run at LightCycler 480 (Roche, Germany) with the cycling conditions indicated in Table 3.6.

Reverse transcription reaction		50°C	30 minutes
Pre-incubation		95°C	15 minutes
Amplification (40 cycles)	Denaturation	94°C	15 seconds
	Annealing	55°C	30 seconds
	Extension	72°C	30 seconds
Cooling		40°C	30 seconds

Table 3.6. PCR cycling conditions.

Data acquisition was performed at the end of each extension step. Obtained C_T values of target gene were normalized to expression of the housekeeping gene *GAPDH* and the fold change was relatively quantified by $2^{-\Delta\Delta CT}$ method [113].

3.2.7. Immunofluorescence

3.2.7.1. Staining of subcellular structures

Breast cancer cells ($3x10^4$ cells/well) were seeded on sterile coverslips (Jena Biosciences circular cover slide 0.22mm, CSL104) that were placed in 12-well plate. After cells were attached on the coverslips, mitochondria and endoplasmic reticulum were stained with Mito-Tracker Red and ER-Tracker Red dyes, respectively. The final concentration of Mito-Tracker Red was determined as 100nM and the concentration was 500nM for ER-Tracker Red. The dyes were given to cells and cells were incubated in 37°C. Incubation times of dyes were set as 5 minutes for Mito-Tracker Red and 15 minutes for ER-Tracker Red.

3.2.7.2. Fixation and permeabilization

After organelle staining, cells were washed with 1X PBS for 10 minutes. Washing was repeated three times. Then, cells were fixed with 4% PFA (paraformaldehyde) solution for 10 minutes and washing steps were followed. For permeabilization of cell membrane, 0.5% Triton X-100 was given and incubated for 5 minutes. Then, cells were washed again as it is described before.

3.2.7.3. Blocking, antibody incubations and mounting

Before antibody incubation, cells were blocked with 0.1% Blocking solution on a shaker for 30 minutes. Then, primary antibody CANT1 was prepared as 1 µg/µl in blocking solution and incubated overnight at 4°C. After 16 hours, 10 minutes wash with 1X PBS was repeated three times. Secondary antibody Alexa Fluor® 488 was prepared and incubated at dark for 1 hour. After washing of secondary antibody, DAPI staining of cell nuclei was carried out on a shaker for 10 minutes and required washes were followed. Cells were mounted with mounting solution on the microscope slides, and coverslip was sealed with transparent nail polish.

3.2.7.4. Confocal imaging

Immunostained cells were visualized by Zeiss LSM 710 Confocal Microscope. Observation and image capture was done through 63x oil immersion objective. Lasers used to excite fluorophores and excitation-emission maxima of fluorophores used in imaging are given in Table 3.7.

Stain/Channel	Excitation maxima	Emission maxima	Laser
DAPI	405nm	459nm	UV Laser
Alexa Fluor® 488	488nm	530nm	Argon Laser
ER-Tracker Red	587nm	615nm	DPSS 561-10 Laser
Mito-Tracker Red	560nm	630nm	DPSS 561-10 Laser

Table 3.7. Fluorophores, their excitation-emission maxima, and the lasers used to excite these fluorophores.

3.2.7.5. Post-processing and colocalization analysis

Captured images were saved as .lsm file. Post-processing was conducted in ZEN software (Blue edition 2.3). Images in .lsm format were split into three channels and then converted into .tiff format in ZEN Blue software. Confocal images in .tiff format were analyzed by CoLocalizer Pro (3.0.2) software in order to quantify colocalization. In colocalization analysis, signal intensity of pixels in channels was detected, and Pearson's coefficient (R_r) and Manders' overlap coefficient (R) were calculated to evaluate colocalization of two channels (red-green) [114].

3.2.8. Statistical Analysis

Quantified results are expressed as mean ± SEM values. Statistical significance of the results was analyzed by the Student's t-tail test, and *P<0.05, **P<0.01 and ***P<0.001 were considered statistically significant.

4. RESULTS

4.1. CANT1 Protein Expression Screening of Breast Cancer Cell Line Panel

Total of forty breast cancer cell lines, four normal breast epithelial cell lines from ATCC breast cancer cell line panel (Appendix F) were screened to detect CANT1 protein expression level endogenously. Prostate cancer cell line PC3 was also involved in this screening because it was previously reported that CANT1 is one of the upregulated genes in prostate cancer [100, 110]. Proteins are collected from total forty-five cell lines, as it was described in the Methods section. 30 μg of total protein loaded and run for each cell line. Protein expressions were analyzed by western blot (Figure 4.1). Anti-CANT1 monoclonal antibody (C-3, sc-515574, Santa Cruz Biotechnology) was used for immunodetection of CANT1 protein. Obtained CANT1 bands possessed different expression patterns, and CANT1 signals varied with a range of 40-45 kDa among cell lines.

According to the results of screening, we decided to continue our studies with MCF7, SK-BR-3 and MDA-MB-468 cells. SK-BR-3 was one of the cell lines that express CANT1 protein highly in western blot results. We then chose MCF7 and MDA-MB-468 cells that have relatively less CANT1 protein levels. Additionally, to consider their receptor status, HER2 (human epidermal growth factor receptor 2) is overexpressed in SK-BR-3. On the other hand, SK-BR-3 is estrogen receptor negative (ER-) but MCF7 is an estrogen receptor-positive (ER+) cell line. MCF7 also has a highly active progesterone receptor (PR) gene. More, MDA-MB-468 is reported as a triple negative cell line that does not express ER, HER2 and PR [115, 116, 117]. As a result, we have representatives from three different groups of breast cancer cell lines classification for our further experiments: HER2+, ER-, PR- (SK-BR-3), HER2-, ER+, PR+ (MCF7) and HER2-, ER-, PR- (MDA-MB-468).

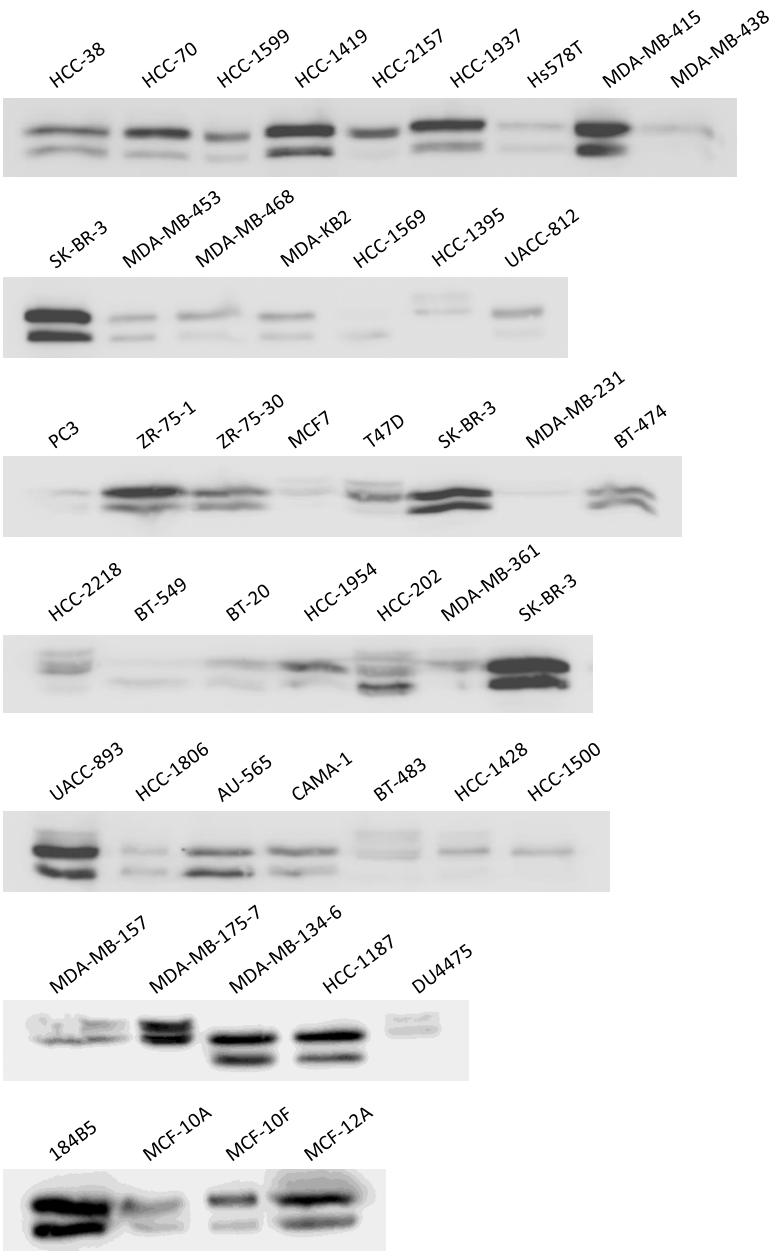

Figure 4.1. Screening the expression of CANT1 in protein level. Forty breast cancer cell lines, four normal breast epithelial cells (184B5, MCF-10A, MCF-10F, MCF-12A) from ATCC breast cancer cell panel and prostate cancer cell line PC3 were screened to detect endogenous CANT1 protein levels. 30 μg total protein extract loaded into 12% gel for each cell line and protein expression levels were analyzed by immunoblotting. Molecular weight of detected CANT1 signals varies between 40-45 kDa.

4.2. Effect of Thapsigargin Concentration and Exposure Time on Cell Death in Breast Cancer Cell Lines

Selected three cell lines, MCF7, SK-BR-3, MDA-MB-468, were treated with THG in dose- or time-dependent manner. Effect of THG on cell viability of three different cell lines was determined by WST-1 Cell Proliferation Assay (Roche). Mean values of obtained viability results are expressed as percentage in Figure 4.2 for dose-dependent and in Figure 4.3 for time-dependent treatments. In the dose-dependent case, even the lowest concentration (10nM) of THG caused a sharp reduction in the viabilities of three cell lines by comparing to their control conditions. The highest concentration (1μM) of THG showed the lowest viability for all cell lines (Figure 4.2).

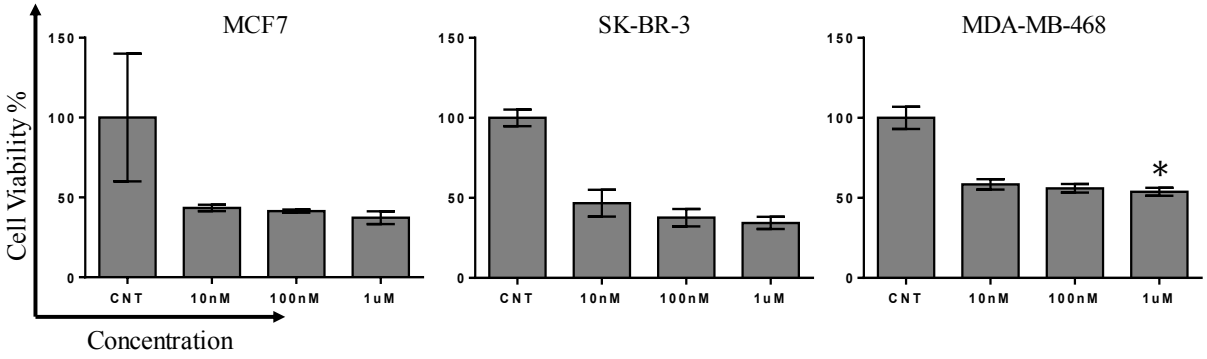

Figure 4.2. Dose-dependent effect of THG treatment. Cells were seeded as 4000 cell/well for three different cell lines and treated with THG for 48 hours with indicated concentrations. Cell viability was measured by WST-1 Cell Proliferation assay (Roche) according to manufacturer's protocol. Histogram results represent the mean values ± SEM. Viability value of control condition (CNT, no treatment) was taken as 100 and remaining values were calculated accordingly. *P<0.05 versus CNT.

Increasing time of THG exposure (4, 8, 16, 24 and 48 hours) revealed a gradually decrease in viability of MCF7, SK-BR-3 and MDA-MB-468 cells (Figure 4.3). All cell viability results indicate that THG has a lethal effect in different concentrations and exposure times for three cell lines. Thus, we determined the THG dose and exposure times which we will perform in our future experiments.

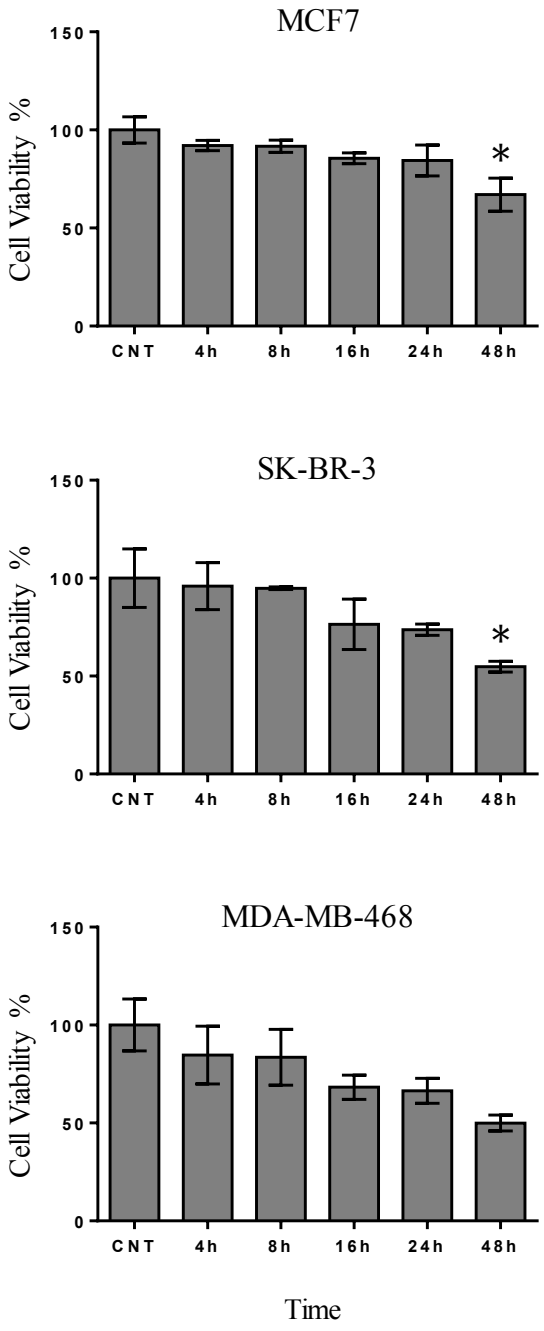

Figure 4.3. Time-dependent effect of THG treatment. Cells were seeded as 4000 cell/well for three different cell lines and treated with THG for 4h, 8h, 16h, 24h and 48h with 100nM final concentration of THG. Cell viability was measured by WST-1 Cell Proliferation assay (Roche) according to manufacturer's protocol. Histogram results represent the mean values ± SEM. Control condition (CNT, no treatment) was taken as 100% viable and other values were set to their corresponded percentages, accordingly. *P<0.05 versus CNT.

4.3. Regulation of CANT1 Protein Expression by Thapsigargin

CANT1 is an ER-located protein [103]. Since Thapsigargin causes ER stress by disrupting Ca^{+2} homeostasis in ER [29], and CANT1 uses Ca^{+2} as an activator for its enzymatic status [100], we wanted to learn if THG treatment in different concentrations and time periods has an effect on CANT1 protein expression level in MCF7, SK-BR-3 and MDA-MB-468 cells. Therefore, immunoblotting experiments were conducted.

4.3.1. Dose-dependent Effect of THG on CANT1 Protein Expression Level

Three different concentrations (10nM, 100nM and 1μM) of THG were tested for 48 hours in three different cell lines. CANT1 signals in blots were normalized according to their corresponded Actin bands in ImageJ software (Figure 4.4). As results of normalization were indicated in histograms, CANT1 protein level was gradually downregulated by increasing doses of THG in MCF7 and MDA-MB-468 cells. However, CANT1 protein expression in SK-BR-3 did not change dramatically and gradually by comparing to the results of other two cell lines.

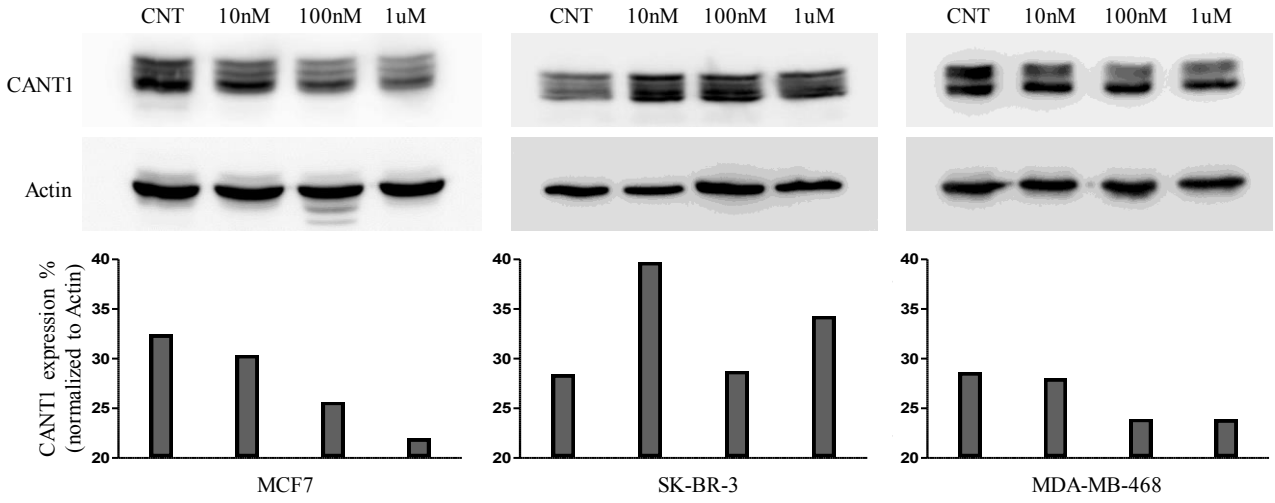

Figure 4.4. Effect of THG with different concentrations on CANT1 protein expression level. MCF7, SK-BR-3 and MDA-MB-468 cells were treated with THG for 48 hours. Final concentrations of THG were indicated. 30 μg total protein was loaded for each cell line. β – Actin is loading control and CNT represents untreated-control condition. Histograms show the percentage of CANT1 protein expression level which was normalized to corresponded

Actin expression level. Molecular weight of Actin and CANT1 is 43 kDa and 40-45 kDa, respectively.

4.3.2. Time-dependent Effect of THG on CANT1 Protein Expression Level

After we obtained the results which indicate THG is able to change the expression behavior of CANT1 in protein level, we decided to observe whether the duration of THG exposure changes CANT1 protein expression level. Therefore, MCF7, SK-BR-3 and MDA-MB-468 cells were treated with THG (C_{final}=100nM) for time periods of 4h, 8h, 16h, 24h and 48h. CANT1 signals in blots were normalized according to their corresponded Actin bands by ImageJ software. Normalized CANT1 protein expression results are shown in histograms (Figure 4.5). As a result, CANT1 protein level reduced gradually by increased exposure time of THG in MCF-7 and MDA-MB-468 cells, and maximum reduction in protein levels were detected in 48h for both cell lines. The change of protein level in SK-BR-3 did not follow a regular pattern.

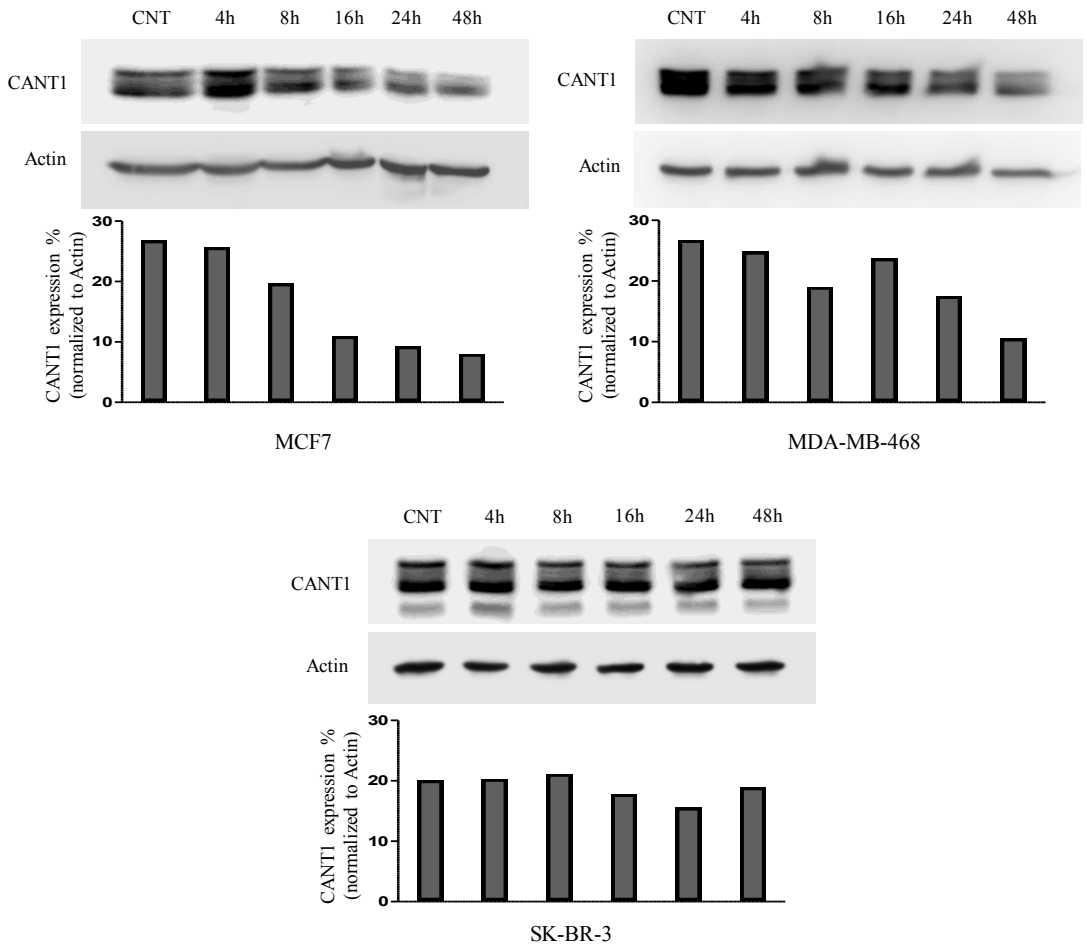

Figure 4.5. Effect of exposure time of THG on CANT1 protein expression level. MCF7, SK-BR-3 and MDA-MB-468 cells were treated with THG (C_{final}=100nM) for 4, 8, 16, 24 and 48 hours. 30 µg total protein was loaded for each cell line. CNT represents untreated-control condition. Histograms show the percentage of CANT1 protein expression which was normalized to corresponded Actin (loading control) expression levels. Molecular weight of Actin and CANT1 is 43 kDa and 40-45 kDa, respectively.

4.4. Effect of Thapsigargin on the Expression of CANT1 mRNA

Since THG can change CANT1 protein expression pattern in both dose- and time-dependent manner, next step was to check if THG can alter the expression of CANT1 mRNA. THG (100nM) was given to cells for 4h, 8h, 16h, 24h and 48h time periods. Total RNA of six different conditions from three cell lines were collected, and real-time RT-PCR experiments were carried out for gene expression quantification. The housekeeping gene *GAPDH* was used as a control. The target gene expressions were normalized by GAPDH expression levels.

Histograms show the fold change of relatively quantified CANT1 mRNA expression levels of three independently performed experiments (Figure 4.6). The significance of fluctuations in mRNA levels were tested statistically. Test results did not indicate any significant change in MCF7 and MDA-MB-468 cells. Only the fold change between the control and 48h THG treatment in SK-BR-3 cells is considered as significant ($p<0.01$).

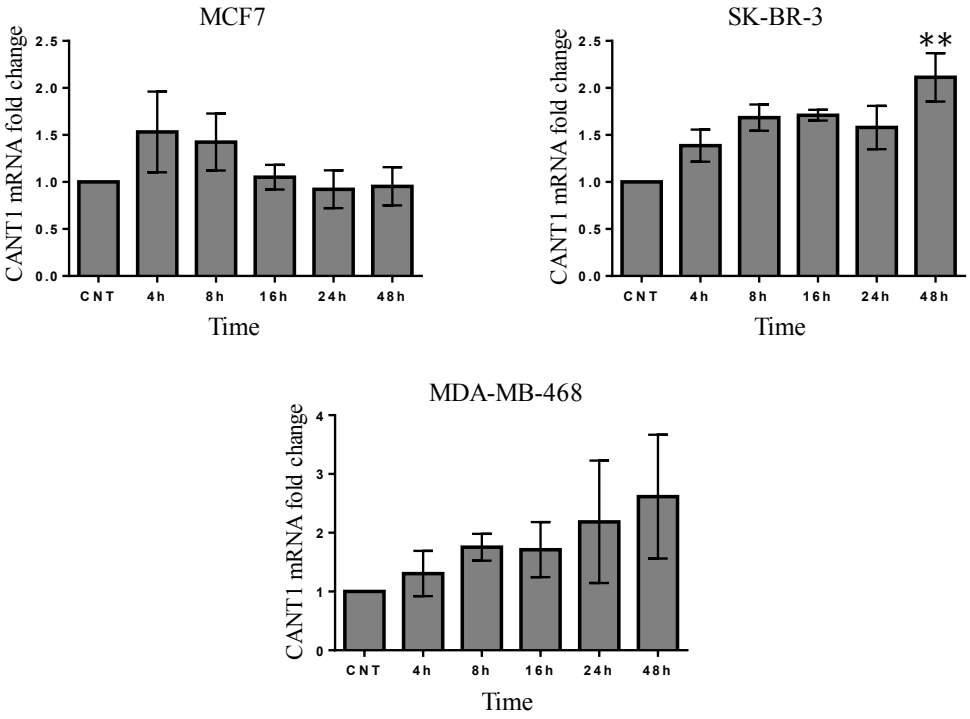

Figure 4.6. Effect of THG on the expression of CANT1 mRNA. Cells were treated with THG (C_{final}=100nM) for various time periods. Total RNAs from each cell line were isolated and real-time RT-PCR was performed to analyze CANT1 gene expression. GAPDH was used as a housekeeping control to normalize corresponded CANT1 levels. CNT is untreated-control condition. Histograms expresses the mean values (± SEM) of three independent experiments for each cell line; **P<0.01 versus control condition.

4.5. Subcellular Localization of CANT1 Protein in Breast Cancer Cell Lines

It was previously reported that CANT1 is an ER-resident protein [103]. To observe the subcellular localization of CANT1 protein in MCF7, SK-BR-3 and MDA-MB-468 cells, we conducted immunofluorescence experiments. We stained mitochondria (Figure 4.7) and endoplasmic reticulum (Figure 4.8) to identify the intracellular distribution of CANT1 protein in breast cancer cells. Then, other steps of immunofluorescence were performed as it

is described in Methods section. Immunodetection of CANT1 protein was provided by a secondary antibody conjugated to Alexa Fluor 488 fluorochrome and displayed in green channel.

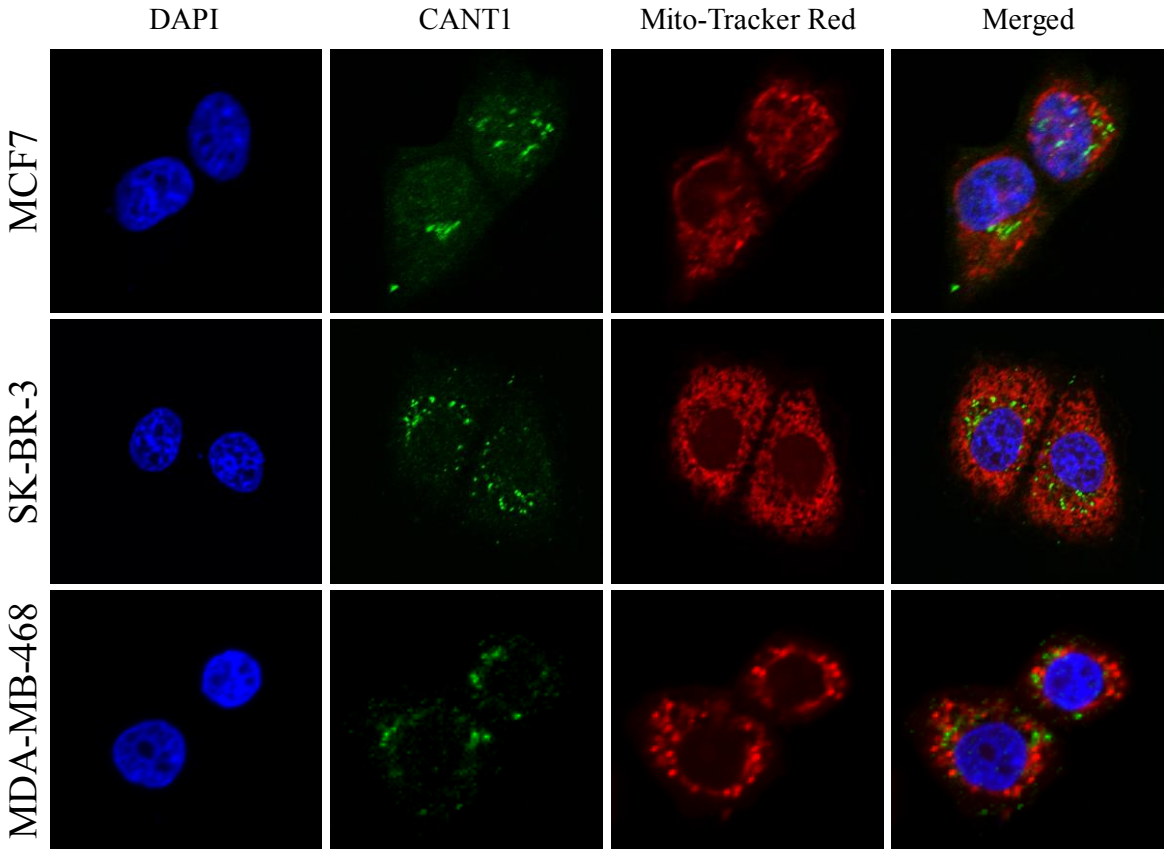

Figure 4.7. Mitochondria staining to observe subcellular localization of CANT1 protein in MCF7, SK-BR-3 and MDA-MB-468 cells. Immunostaining of cells were performed to observe intracellular position of CANT1 protein. Mitochondria (red) and nucleus (blue) were stained with Mito-Tracker Red (C_{final}=100nM) and DAPI, respectively. The staining of CANT1 protein was followed by secondary antibody conjugated to Alexa Fluor 488 fluorochrome. Images were taken by 63x objective in confocal laser scanning microscope.

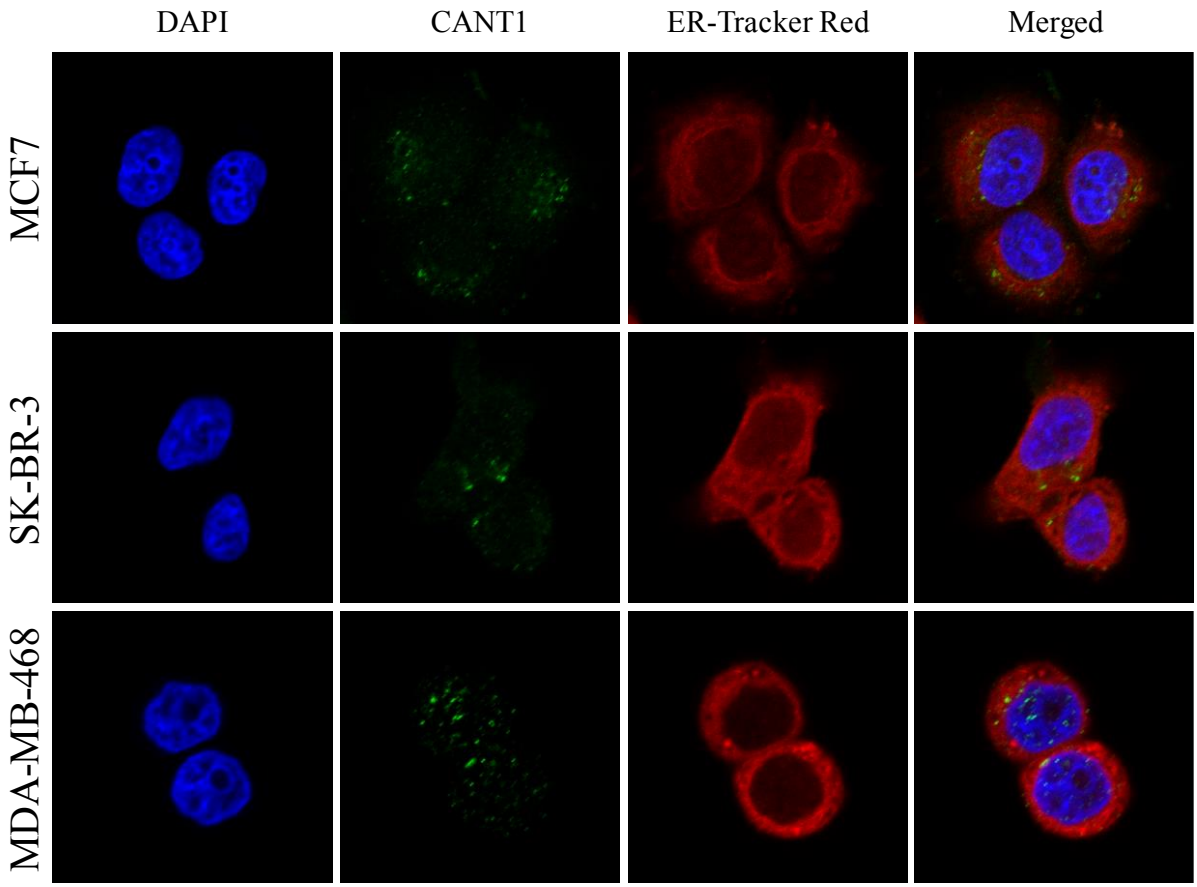

Figure 4.8. Endoplasmic reticulum staining to observe subcellular localization of CANT1 in MCF7, SK-BR-3 and MDA-MB-468 cells. Immunostaining of cells was performed to observe intracellular position of CANT1 protein. Endoplasmic reticulum (red) and nucleus (blue) were stained with ER-Tracker Red (C_{final}=500nM) and DAPI, respectively. The staining of CANT1 protein was followed by secondary antibody conjugated to Alexa Fluor 488 fluorochrome. Images were taken by 63x objective in confocal laser scanning microscope.

4.6. Examining Intracellular Localization of CANT1 Protein Under Thapsigargin Exposure

Disruption of ER homeostasis is followed by activation of ER stress [9]. We induced ER stress with THG, and we observed changes in CANT1 expression in protein level. However, we also wanted to learn how CANT1 localization can be affected during ER stress activation. To answer this question, we treated breast cancer cells with THG for 4 hours and 8 hours, and we monitored and analyzed subcellular localization of CANT1 protein due to THG treatment.

4.6.1. Effect of Thapsigargin on CANT1-Mitochondria Colocalization

First, we examined CANT1-mitochondria colocalization. THG (C_{final}=100nM) was given to MCF7, SK-BR-3 and MDA-MB-468 cells for 4 hours and 8 hours. Mitochondria was stained with MitoTracker Red (C_{final}=100nM). Immunofluorescence protocol was followed and CANT1 protein was detected with secondary antibody conjugated to Alexa Fluor 488. Images were captured in confocal laser scanning microscope. Colocalization of CANT1 and mitochondria were analyzed in CoLocalizer Pro software as two channels, green channel for CANT1 and red channel for mitochondria. Merged channels and pixel scatter-grams are shown in Figure 4.9. Analysis results revealed two different coefficient, Pearson's Correlation Coefficient (Rr) and Manders' Overlap Coefficient (R) (Table 4.1), which calculates pixel densities of two channel and gives colocalization ratio [114]. Mean values ± SEM of Manders' Overlap Coefficient for three cell lines were displayed in histograms in Figure 4.10. Statistical tests were conducted to compare difference between mean values of control and treatment conditions in MCF7, SK-BR-3 and MDA-MB-468 cell lines, however one-way ANOVA test did not indicate any significant difference ($P>0.05$). Consequently, THG treatment did not affect the change in the colocalization of CANT1 and mitochondria significantly.

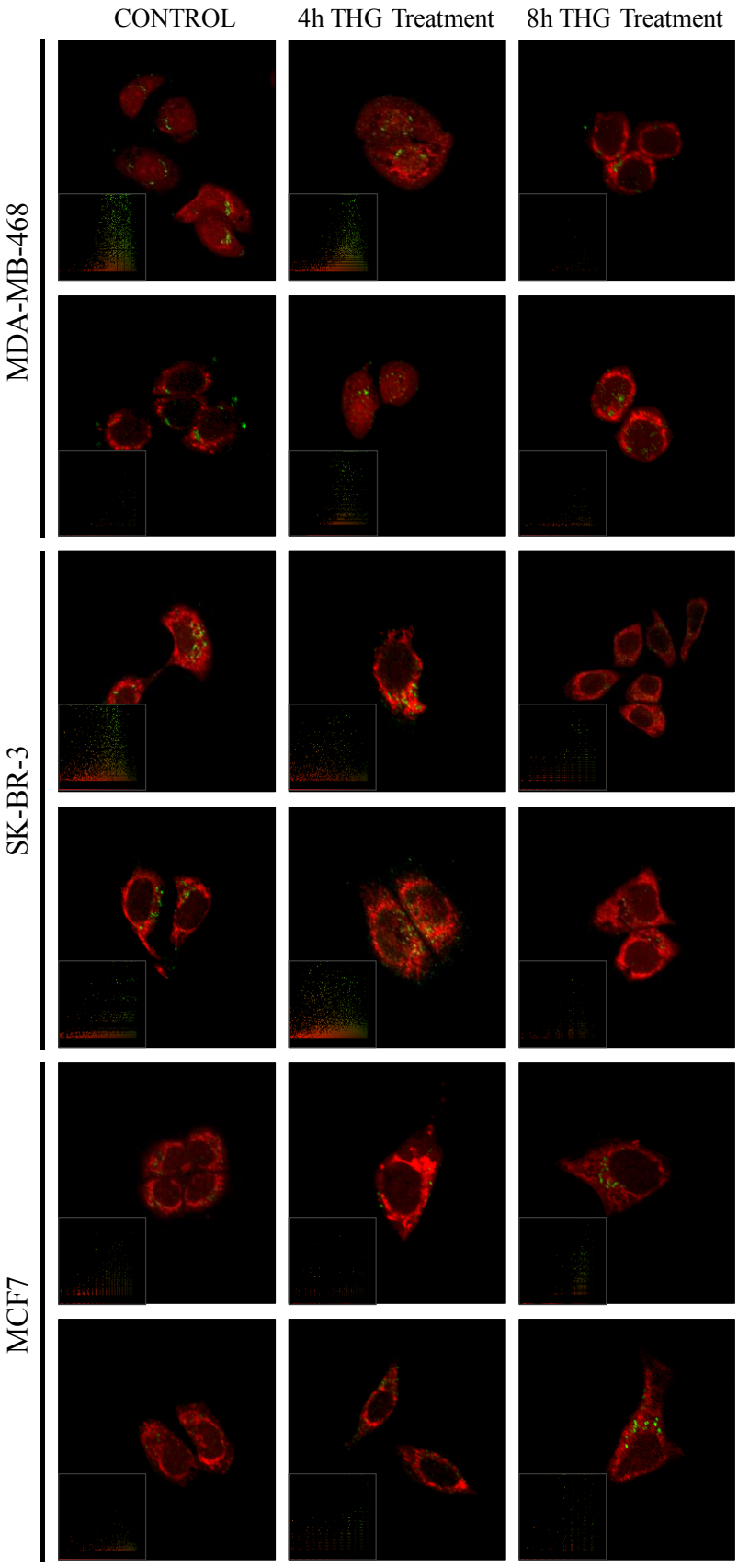

Figure 4.9. Colocalization analysis of CANT1 and mitochondria in MCF7, SK-BR-3 and MDA-MB-468 cells. THG (C_{final}=100nM) was given to three different cells for 4 hours or 8 hours. Confocal images were taken by 63x objective in laser scanning microscope. Colocalization analysis of CANT1 (green) and mitochondria (red) was performed by CoLocalizer Pro software. Scatter-grams were placed upper-left of each image. CNT indicates untreated cells.

CANT1-Mitochondria Colocalization	**THG treatment**	**Pearson's Correlation Coefficient (Rr)**	**Manders' Overlap Coefficient (R)**
MCF7	No treatment	-0.0074	0.2381
		0.1556	0.2933
		-0.0170	0.3317
	4h THG treatment	-0.0018	0.2923
		-0.0024	0.0834
		-0.0343	0.0908
		0.1284	0.2603
		0.0308	0.1277
		0.1271	0.1546
	8h THG treatment	0.0608	0.1881
		-0.0802	0.3729
		-0.1162	0.2661
		-0.0895	0.2855
		-0.1329	0.2521
		0.0712	0.2198
SK-BR-3	No treatment	-0.0388	0.1728
		0.0695	0.3219
		0.0335	0.3328
		0.0784	0.3170
		-0.1515	0.2509
		0.0232	0.2951
	4h THG treatment	0.1519	0.5487
		-0.0550	0.4715
		0.0544	0.4032
		0.2557	0.4689
	8h THG treatment	0.1575	0.5350
		0.0797	0.3595
		0.0787	0.2311
		0.0500	0.1465
		0.1809	0.5434

MDA-MB-468	No treatment	0.0382	0.1695
		0.0474	0.2217
		0.1083	0.2197
		-0.0487	0.1682
		0.1030	0.3385
	4h THG treatment	0.1380	0.3946
		0.0888	0.2869
		0.0663	0.2458
	8h THG treatment	0.0714	0.1865
		0.1445	0.3702
		0.0269	0.1088
		0.0565	0.3277

Table 4.1. Pearson's Correlation Coefficient (Rr) and Manders' Overlap Coefficient (R) that were revealed by colocalization analysis of CANT1 and mitochondria.

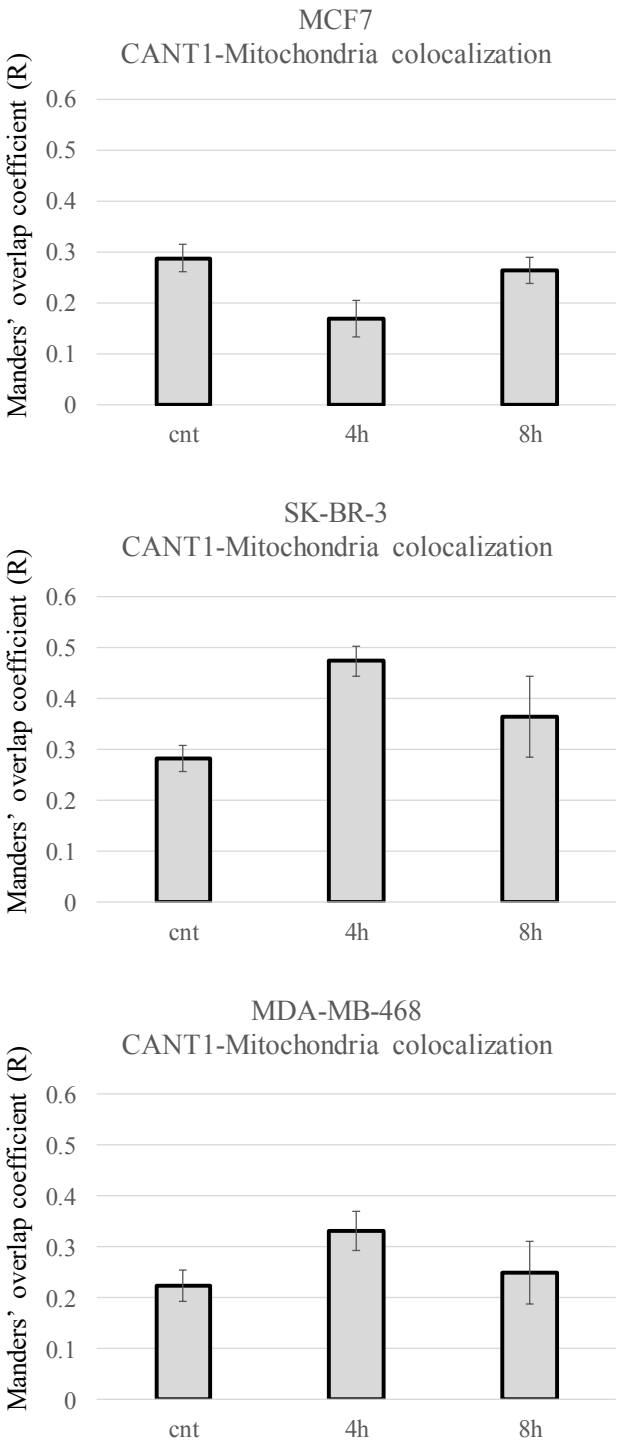

Figure 4.10. Colocalization of CANT1 and mitochondria according to Manders' Overlap Coefficient. MCF7, SK-BR-3 and MDA-MB-468 cells were treated with THG (C_{final}=100nM) for 4 hours and 8 hours. Colocalization was analyzed by CoLocalizer Pro software and, analysis revealed Manders' Overlap Coefficient values. Histograms show mean value ± SEM of Manders' Overlap Coefficient. CNT is untreated-control condition.

4.6.2. Effect of Thapsigargin on CANT1-Endoplasmic Reticulum Colocalization

Next, we studied CANT1-ER colocalization pattern under THG exposure. After cells treated with THG (C_{final}=100nM) for 4 hours and 8 hours, ER was stained with ER-Tracker Red (C_{final}=500nM), and immunofluorescence protocol was followed. CANT1 protein was detected with secondary antibody conjugated to Alexa Fluor 488 fluorochrome. Confocal images were photographed in laser scanning microscope and they were analyzed by CoLocalizer Pro software. Colocalization analysis was performed by measuring pixel densities of two channels, green channel (CANT1) and red channel (ER). Merged channels with pixel scatter-grams were shown in Figure 4.11 for MCF7, in Figure 4.12 for SK-BR-3 and in Figure 4.13 MDA-MB-468 cells. Colocalization coefficients were listed in Table 4.2. Quantification of Manders' Overlap Coefficient for three cell lines were displayed in histograms (Figure 4.14.). Here, statistical tests were conducted to detect significance in differences between conditions (CNT, 4h, 8h). According to the results of statistical tests, CANT1 and ER colocalization changes in MCF7 and MDA-MB-468 cell lines significantly due to THG treatment (*$P<0.05$, **$P<0.01$ and ***$P<0.001$). THG treatment did not exhibit any significant effect on the change of CANT1-ER colocalization in SK-BR-3 cell line ($P>0.05$).

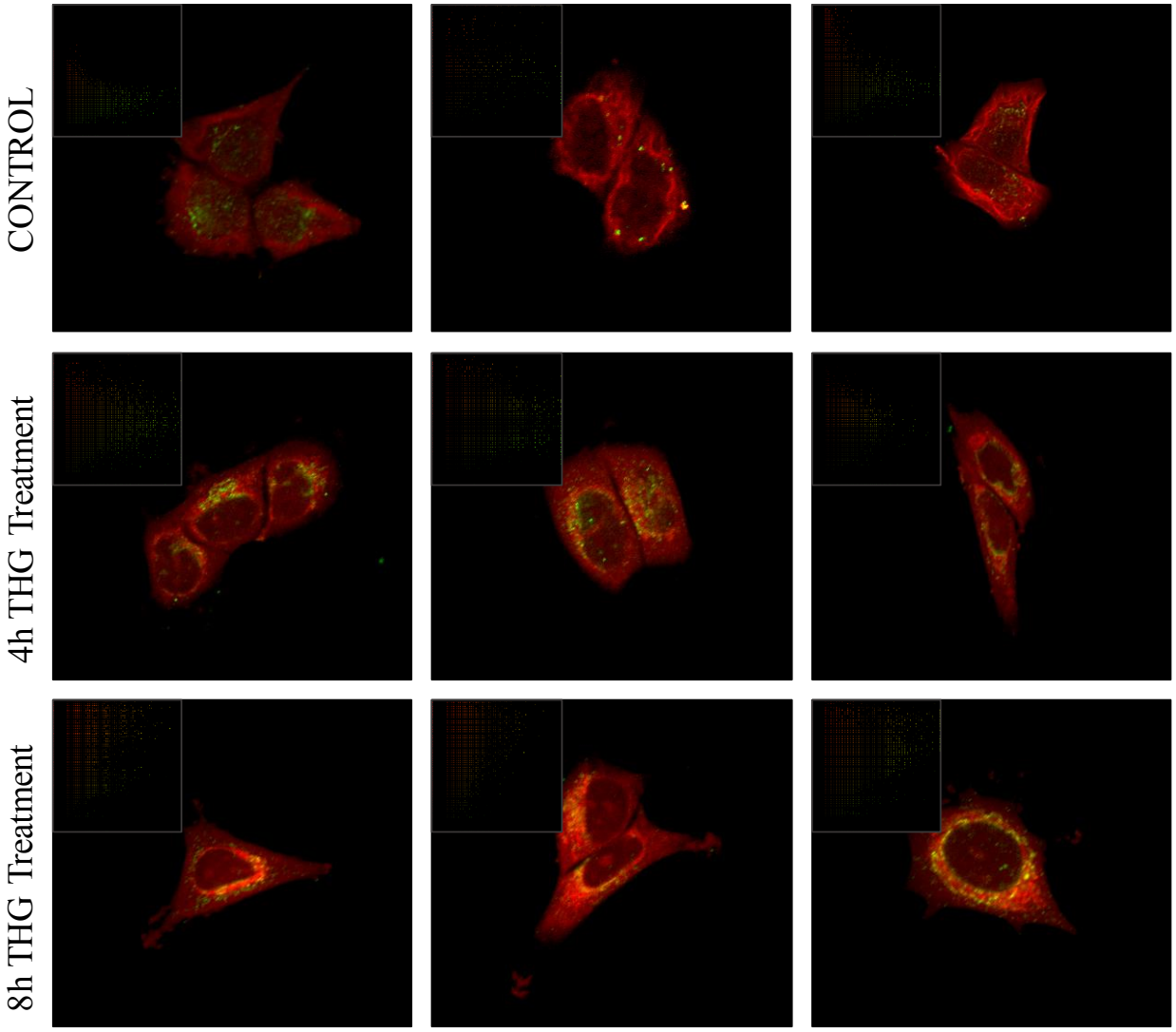

Figure 4.11. CANT1-ER colocalization analysis in MCF7 cells. Cells were treated with THG (C_{final}=100nM) for 4 hours or 8 hours. Confocal images were taken by 63x objective in laser scanning microscope. Colocalization analysis of CANT1 (green) and ER (red) was performed by CoLocalizer Pro software. Scatter-grams were placed upper-left of each image. CNT indicates untreated cells.

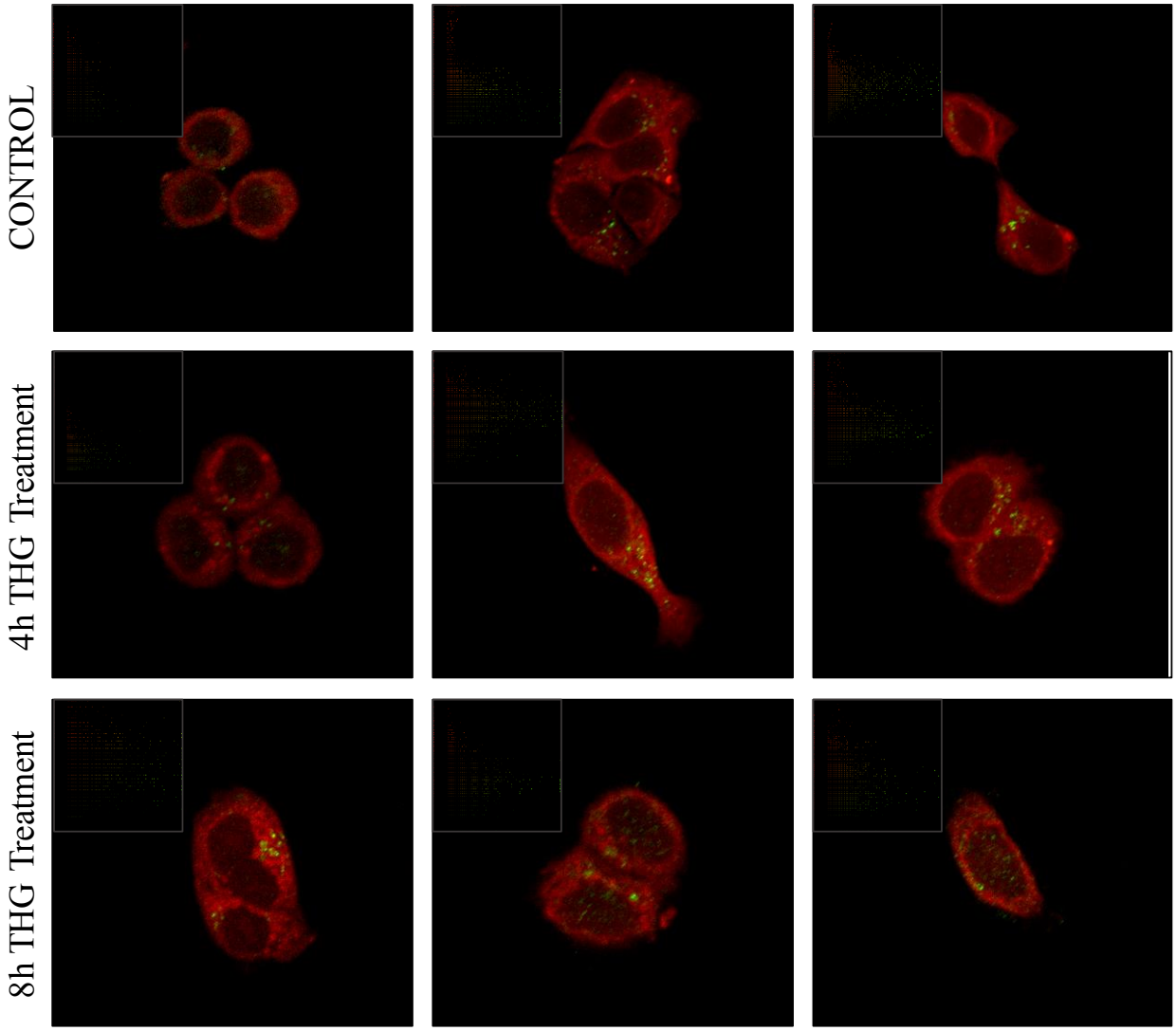

Figure 4.12. CANT1-ER colocalization analysis in SK-BR-3 cells. Cells were treated with THG (C_{final}=100nM) for 4 hours or 8 hours. Confocal images were taken by 63x objective in laser scanning microscope. Colocalization analysis of CANT1 (green) and ER (red) was performed by CoLocalizer Pro software. Scatter-grams were placed upper-left of each image. CNT indicates untreated cells.

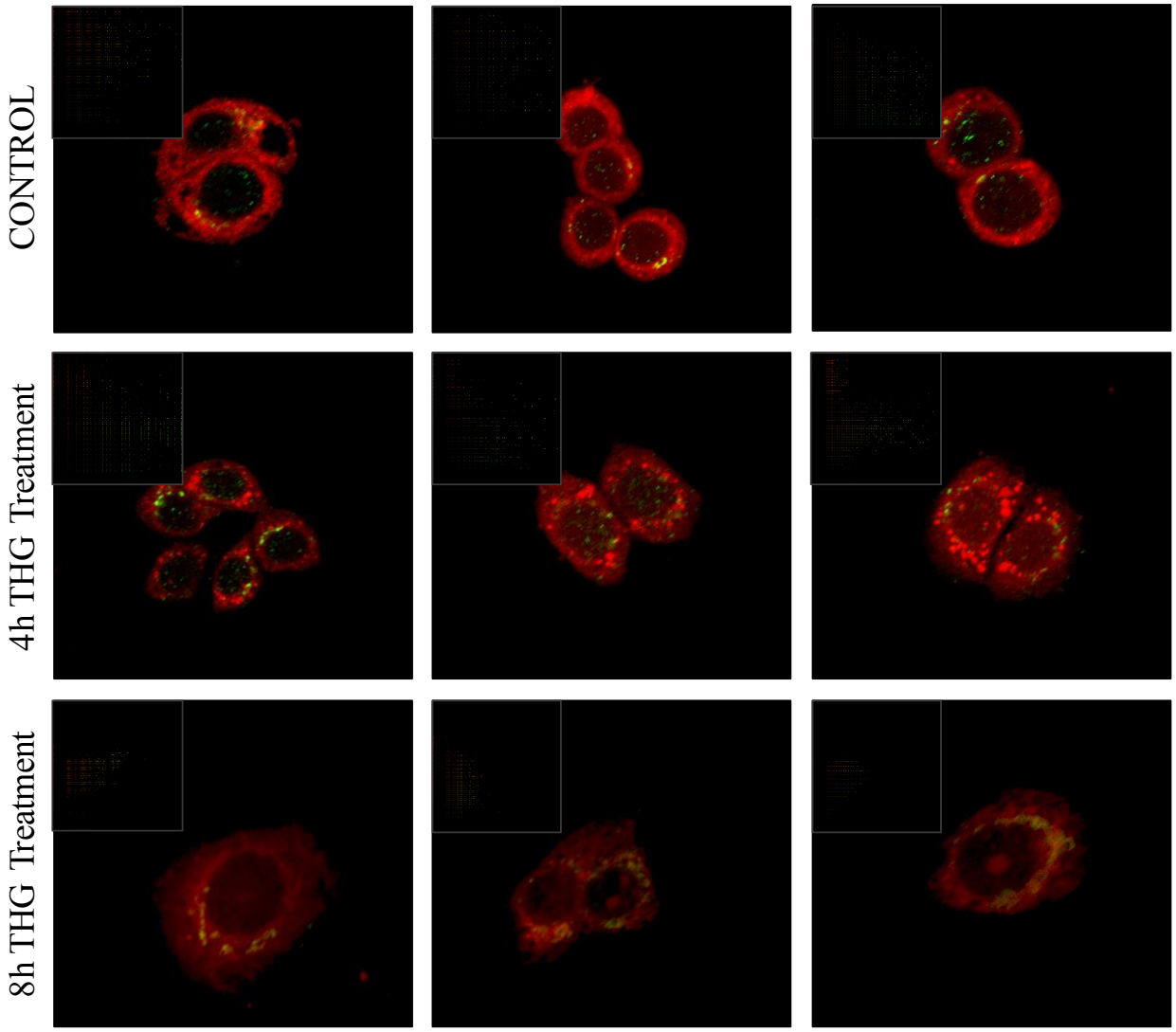

Figure 4.13. CANT1-ER colocalization analysis in MDA-MB-468 cells. Cells were treated with THG (C_{final}=100nM) for 4 hours or 8 hours. Confocal images were taken by 63x objective in laser scanning microscope. Colocalization analysis of CANT1 (green) and ER (red) was performed by CoLocalizer Pro software. Scatter-grams were placed upper-left of each image. CNT indicates untreated cells.

CANT1-ER Colocalization	**THG treatment**	**Pearson's Correlation Coefficient (Rr)**	**Manders' Overlap Coefficient (R)**
MCF7	No treatment	0.0559	0.4157
		0.1018	0.5777
		0.2009	0.4686
		-0.1759	0.2883
		0.0556	0.3198
		0.1874	0.1923
		0.1394	0.4011
	4h THG treatment	0.2595	0.4430
		0.4800	0.6086
		0.4260	0.5073
		0.4049	0.6105
		0.3371	0.4820
	8h THG treatment	0.4049	0.6105
		0.5653	0.5800
		0.4697	0.5004
		0.6430	0.7222
		0.6102	0.6959
SK-BR-3	No treatment	0.0788	0.2247
		0.0286	0.4009
		0.1094	0.2246
		0.0867	0.2164
		0.1612	0.2727
	4h THG treatment	-0.0910	0.1540
		0.1149	0.3779
		0.2775	0.2973
		0.2809	0.3151
		0.3472	0.4720
		0.0867	0.2164
	8h THG treatment	0.1899	0.2733
		0.0640	0.2766

SK-BR-3	8h THG treatment	0.1169	0.3880
		0.1177	0.4781
		0.1801	0.5904
MDA-MB-468	No treatment	0.0728	0.3365
		0.1034	0.2110
		-0.0339	0.1877
		-0.0559	0.1084
		0.0287	0.1494
		-0.0673	0.2117
		-0.0052	0.1899
		0.1693	0.1843
		0.1532	0.1943
	4h THG treatment	0.0610	0.3308
		0.0240	0.1608
		-0.1431	0.1970
		0.0500	0.3880
		0.1544	0.3571
		0.1250	0.3334
	8h THG treatment	0.4247	0.6217
		0.5740	0.4265
		0.3313	0.2892
		0.5965	0.5595
		0.4059	0.4628
		0.4309	0.3207

Table 4.2. Pearson's Correlation Coefficient (Rr) and Manders' Overlap Coefficient (R) that were revealed by colocalization analysis of CANT1 and endoplasmic reticulum.

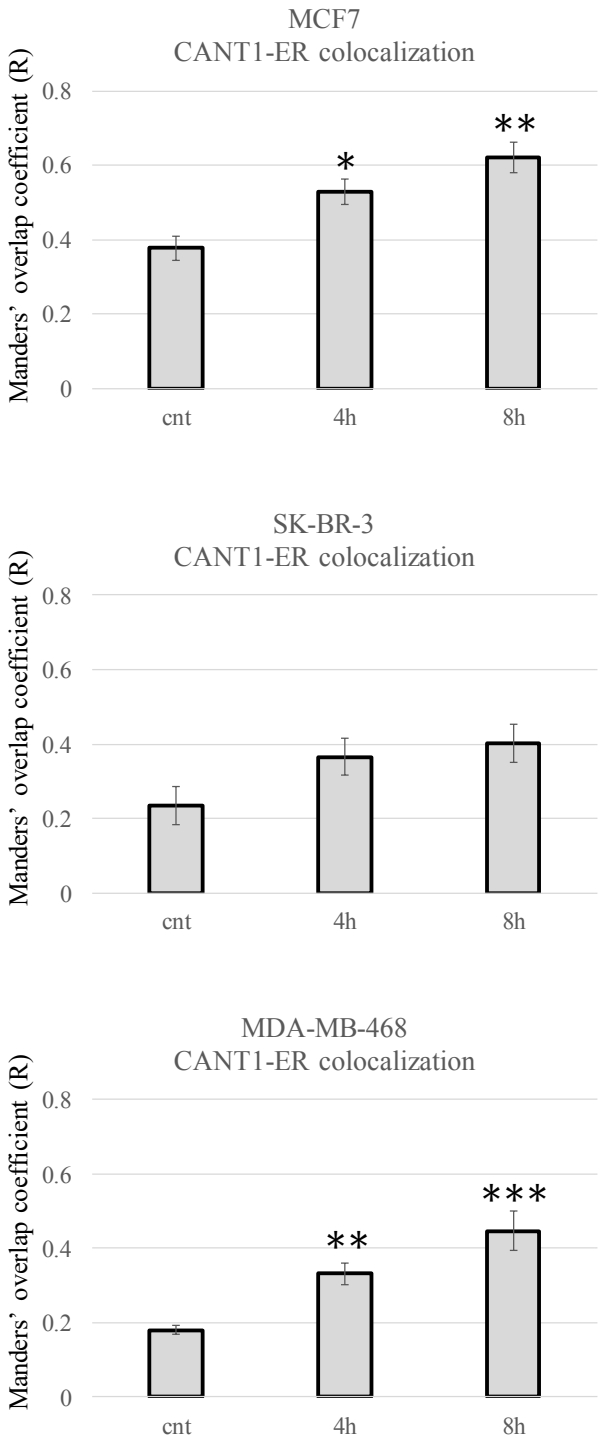

Figure 4.14. Colocalization of CANT1 and endoplasmic reticulum according to Manders' Overlap Coefficient. MCF7, SK-BR-3 and MDA-MB-468 cells were treated with THG (C_{final}=100nM) for 4 hours and 8 hours. CNT is untreated-control condition. Colocalization was analyzed by CoLocalizer Pro software, and analysis revealed Manders' Overlap Coefficient values. Histograms show mean value ± SEM of Manders' Overlap Coefficient; *P<0.05, **P<0.01 and ***P<0.001 versus control condition.

5. DISCUSSION

The ER has fundamental roles in the cell, such as translation, protein modification, protein quality control, secretion of proteins, lipid biosynthesis and calcium storage. Maintenance of ER homeostasis is required for cell health and survival [1]. ER mechanisms can be affected by external and internal factors that disrupts ER homeostasis and cause ER stress. The protective mechanism unfolded protein response (UPR) is activated to manage ER stress. If the stress does not exceed, UPR handles this stress and reestablishes ER homeostasis back to contribute to cell survival. However, if the stress is prolonged and causes severe damage, UPR downstream activates apoptotic cell death signaling [9, 10] .

Calcium-activated nucleotidase 1 (CANT1) is a nucleotide hydrolyzing enzyme which belongs to apyrase family. It is responsible for the converting of extracellular nucleoside di- and triphosphates into nucleoside monophosphates [100]. The mutation in CANT1 gene is associated to Desbuquois dysplasia which is an autosomal recessive disorder revealing skeletal growth abnormalities in joints, hands and femur [104, 105]. The role of CANT1 in Desbuquois dysplasia in not unclear but there is a proposed mechanism about the involvement of CANT1 in the proteoglycan metabolism in the case of Desbuquois dysplasia [107].

In human, prostate is one of the tissues in which CANT1 mRNA is expressed highly [100]. Upon this knowledge, the expression and regulation of CANT1 has been studied previously in the prostate cancer cells [109, 110]. CANT1 expression in breast cancer cells was mentioned in one study indicating CANT1, as a phosphatase, is under-expressed in the estrogen negative breast cancer cell lines in comparison to estrogen positive cell lines [118]. In the construction of this thesis, we aimed to identify the regulation of CANT1 in breast cancer cell lines during ER stress-induced cell death.

Firstly, in order to have an idea about the expression of CANT1 protein in breast cancer cell lines, we screened forty breast cancer cell lines, four normal breast epithelial cell lines and

one prostate cancer cell line (PC3) to analyze CANT1 protein expression patterns by immunoblotting (Figure 4.1). Because it was reported that CANT1 is overexpressed endogenously in prostate cancer [100, 109, 110], we preferred to use it as a positive control. Our screening results revealed different expression patterns. The molecular weight of CANT1 protein was between 40-45 kDa among cell lines. The number of detected band signals was also showed diversity. We observed three separated signals that have different molecular weights from 40 kDa to 45 kDa. The reason of this variety can be that the alternatively spliced forms of CANT1 protein might show different characteristics among cell lines. In other words, different breast cancer cell lines are able to splice CANT1 mRNA differently to generate variant forms of the protein. Another reason of this might be related to post-translation modifications of CANT1 protein. Smith *et al.* showed that CANT1 is a glycosylated protein. They observed that signal of CANT1 shifted to lower kDa in western blot analysis after they deglycosylate the protein by PNGase F [100], meaning that detected signals in different molecular weights can be caused by post-translational modifications. Other post-translational modifications can be investigated to clarify why and how the different number of protein signals with different molecular weight in immunoblot detection were obtained.

In the screening results, CANT1 protein was found to be expressed relatively high in SK-BR-3, HCC-1419, MDA-MB-415, UACC-983, MDA-MB-175-7 and MDA-MB-134-6 cell lines. The expression pattern of these cell lines was two bands with approximately same signal intensity. There are also cell lines such as HCC-70, HCC-202, HCC-1937, HCC-1954, HCC-2157 and ZR-75-1 that have one band signal is more intense than the other band. A third band, the soluble variant of CANT1, has emerged in HCC-202 and HCC-2218 cell lines.

We decided to study with SK-BR-3, MCF7 and MDA-MB-468 for our further experiments. Detected protein levels in MDA-MB-468 and MCF7 cells were relatively less when we compared to those of SK-BR-3. Addition to that, we think the receptors that are expressed on these cell lines might be important because studies showed that CANT1 is an androgen-regulated protein in prostate cancer [109, 110]. Therefore, the hormonal regulation of CANT1 in breast cancer can be operated by receptor expression. HER2, estrogen and progesterone receptor status of these cell lines are HER2+, ER-, PR- for SK-BR-3, HER2-, ER+, PR+ for MCF7 and HER2-, ER-, PR- for MDA-MB-468 [116, 117].

Thapsigargin (THG) was used to generate ER stress. Next step was to determine dose and exposure time of THG in breast cancer cell lines. MCF7, SK-BR-3 and MDA-MB-468 cells were treated with THG in dose-dependent (10nM, 100nM and 1μM) and time dependent manner (4h, 8h, 16h, 24h and 48h). The effect of THG on the viabilities of breast cancer cell lines was assessed by a proliferation assay. In the dose dependent case, even the lowest concentration of THG (10nM) caused the death of almost 50% of the cells in all three cell lines (Figure 4.2). For time-dependent case (Figure 4.3), the increasing exposure time of THG caused a gradual reduction in the viability of three cell lines, as it was expected. However, this reduction of viability among cell lines show variety. For instance, in MCF7 cells, cell viability was detected around 85% from 4h to 24h treatments. However, detected cell viability was decreased to 70% at 48h in MCF7 while SK-BR-3 and MDA-MB-468 cells showed sharper reduction in cell death after 16h of treatment. This is because different cell lines response and progress ER stress-induced apoptotic cell death signaling differently. These differences can be related to the THG exposure time which rules the transition of UPR from cytoprotective mode to killer mode. To elaborate this transition, we can perform additional cell death detection assays in our future works, as in one study examining apoptosis initiation by THG in MCF7 and MDA-MB-468 cell lines [119].

The way that THG cause ER stress is the disruption of calcium homeostasis by inhibiting SERCA pumps which are responsible for the transportation of cytosolic calcium into ER [29]. Since CANT1 is an ER-resident protein, and calcium is responsible for not only enzymatic activation of CANT1 but also the structural stability and conformation [102], we wanted to learn how CANT1 protein level is affected during ER stress-induced cell death. According to the previously determined doses (10nM, 100nM and 1μM; for 48h) and exposure times (4h, 8h, 16h, 24h and 48h; with 100nM) of THG, we treated MCF7, SK-BR-3 and MDA-MB-468 cells and performed immunoblotting experiments to detect protein levels. Figure 4.4 shows the effect of different concentrations of THG on the CANT1 protein expression. Increasing dose of THG caused an apparent reduction of protein levels in MCF7 and MDA-MB-468 cells. However, CANT1 protein level in SK-BR-3 fluctuated and did not follow a regular pattern through ER stress activation.

CANT1 protein was also downregulated in MCF and MDA-MB-468 cell lines by the increased exposure time (Figure 4.5). The regulation of protein level in SK-BR-3 did not

follow a pattern like these of MCF7 and MDA-MB-468 cell lines. Addition to that, SK-BR-3 immunoblot result (Figure 4.5) revealed a third band (36-38 kDa) which is probably the soluble form of CANT1 as it was reported before [100, 101].

In both dose- and time-dependent treatments, CANT1 protein levels in SK-BR-3 cell line did not change dramatically and gradually like two other cell lines. The reason for this case might be related to the protein turnover rate of SK-BR-3 cells. Among three cell lines, SK-BR-3 is the only cell line which expresses HER2 receptor. To answer the question if it is receptor status-dependent or not, CANT1 expression patterns in other HER2+ breast cancer cell lines can be studied in the future.

Since we observed changes in CANT1 protein expression by THG-mediated ER stress, we also wanted to observe how CANT1 mRNA expression levels change upon THG treatment. Cells were treated with THG (100nM) for various time periods. Gene expression quantification of CANT1 was performed and results are shown in Figure 4.6. Obtained data was statistically tested. However, changes in the mRNA expression levels in MCF7 and MDA-MB-468 cell lines are not considered as significant according to statistical tests that we conducted. Only detected significant difference was between the control and 48h treatment of SK-BR-3 cells. Our findings suggest that protein expression alterations are not affected in transcriptional level. Therefore, we can hypothesize that the regulation of CANT1 expression during ER stress is a protein level-dependent process. In our future studies, we would like to focus on the protein processing mechanisms such as translation, post-translational modifications, protein activation and transport.

It is known that CANT1 is an ER-resident protein. Additionally, CANT1 was also detected at ER-Golgi transition regions by immunocytochemical assays [103]. In the Figure 4.7 and Figure 4.8, we stained mitochondria and ER, respectively, and we wanted to observe the subcellular localization of CANT1 in the breast cancer cell lines through the stained organelle references. CANT1 protein is detected in close proximity to nucleus, indicating a localization at ER or ER-Golgi transition sites. However, we also observed the distribution of CANT1 protein across the cell, most probably the fixation and staining steps of immunofluorescence synchronized with translation or transportation processes of the protein in the cell.

After that, we investigated the effect of THG on the subcellular localization of CANT1. Therefore, we conducted colocalization analysis. In Figure 4.9, confocal imaging of CANT1-mitochondria staining as merged channels is shown. Coefficients that were obtained from performed colocalization analysis were statistically tested to determine if the changes upon the treatment are significant or not. Our results suggest that THG does not affect CANT1-mitochondria colocalization significantly (Figure 4.10).

As a next step, ER was stained for colocalization analysis in breast cancer cell lines. Confocal microscopy images of merged channels were shown in Figure 4.11 for MCF7, in Figure 4.12 for SK-BR-3 and in Figure 4.13 MDA-MB-468 cells with pixel scatter-grams. The results of colocalization analysis were quantified (Figure 4.14). We notice that CANT1 and ER colocalization correspondingly revealed an increasing pattern with the increased time of THG exposure. According to the statistical tests that we conducted, the increasing in the colocalization of CANT1 and ER is found significant in MCF7 and MDA-MB-468 cell lines. However, the observed change of CANT1-ER colocalization in SK-BR-3 is not significant ($P>0.05$). The increase in the localization to ER upon stress might offer a role for CANT1 regarding the regulation of UPR since it is reported that APY-1, the *Caenorhabditis elegans* homologue of CANT1, involves in UPR signaling in the nematode [112]. Another study reported that CANT1 may contribute to protein synthesis and degradation, and it may control calcium homeostasis since CANT1 overexpression increases Ca^{+2} level in the Golgi [111]. These suggested roles for CANT1 can present possible functions that are related to ER mechanisms.

In summary, we investigated the regulation of CANT1 in breast cancer cells that undergoing ER stress or initiating apoptotic cell death. We showed that the regulation of CANT1 protein is cell subtype-dependent. In the literature, the number of studies that are related to CANT1 is limited, and also the studies focus on different approaches. Our aim was to identify the role and the regulation of CANT1 protein in breast cancer during ER stress-related cell death, which has not been reported before. This study and the findings have generated many questions for the future of our research. First of all, we would like to clarify the reasons and mechanisms behind the number of protein signal bands detected in our immunoblot results. We can check if this case is related to post-translational modifications or not. If these differences are related to alternative splicing processing, then we can delete exons or intron-

exon junctions by gene editing methods to explain their importance and functions. Furthermore, in order to identify the role of CANT1 in ER or in the cell, we can conduct protein-protein interaction studies. The activation of caspases and UPR downstream elements can be monitored to check the regulation of CANT1 during ER stress-induced cell death. Furthermore, to define a more general role for CANT1, other breast cancer cell subtypes can be studied.

6. REFERENCES

1. Schwarz DS, Blower MD. The endoplasmic reticulum: Structure, function and response to cellular signaling. *Cell Mol Life Sci*. 2016;73(1):79-94. doi:10.1007/s00018-015-2052-6.
2. Braakman I, Hebert DN. Protein folding in the endoplasmic reticulum. *Cold Spring Harb Perspect Biol*. 2013;5(5). doi:10.1101/cshperspect.a013201.
3. Braakman I, Bulleid NJ. Protein Folding and Modification in the Mammalian Endoplasmic Reticulum. *Annu Rev Biochem*. 2011;80(1):71-99. doi:10.1146/annurev-biochem-062209-093836.
4. Ellgaard L, McCaul N, Chatsisvili A, Braakman I. Co- and Post-Translational Protein Folding in the ER. *Traffic*. 2016;17(6):615-638. doi:10.1111/tra.12392.
5. Xu C, Ng DTW. Glycosylation-directed quality control of protein folding. *Nat Rev Mol Cell Biol*. 2015;16(12):742-752. doi:10.1038/nrm4073.
6. Bulleid NJ. Disulfide bond formation in the mammalian endoplasmic reticulum. *Cold Spring Harb Perspect Biol*. 2012;4(11):1-12. doi:10.1101/cshperspect.a013219.
7. Ellgaard, Lars and Helenius A. ER quality control: towards an understanding at the molecular level. *Curr Opin Cell Biol*. 2001;13:431-437.
8. Fagone P, Jackowski S. Membrane phospholipid synthesis and endoplasmic reticulum function. *J Lipid Res*. 2009;50(Supplement):S311-S316. doi:10.1194/jlr.R800049-JLR200.
9. Shen X, Zhang K, Kaufman RJ. The unfolded protein response: A stress signaling pathway of the endoplasmic reticulum. *J Chem Neuroanat*. 2004;28(1-2):79-92. doi:10.1016/j.jchemneu.2004.02.006.
10. Hetz C. The unfolded protein response: Controlling cell fate decisions under ER stress and beyond. *Nat Rev Mol Cell Biol*. 2012;13(2):89-102. doi:10.1038/nrm3270.
11. Gething M. Role and regulation of the ER chaperone BiP. *Cell Dev Biol*. 1999;10:465-472.
12. Walter P, David R. The Unfolded Protein Response: From stress pathway to homeostatic regulation. *Science (80-)*. 2011;334(6059):1081-1086. doi:10.1126/science.1209038.
13. Adachi Y, Yamamoto K, Okada T, Yoshida H, Harada A. ATF6 Is a Transcription Factor Specializing in the Regulation of Quality Control Proteins in the Endoplasmic Reticulum. *Cell Struct Funct*. 2008;33:75-89.
14. Chen X, Shen J, Prywes R. The Luminal Domain of ATF6 Senses Endoplasmic

Reticulum (ER) Stress and Causes Translocation of ATF6 from the ER to the Golgi. *J Biol Chem*. 2002;277(15):13045-13052. doi:10.1074/jbc.M110636200.

15. Sano R. and Reed J. ER stress-induced cell death mechanisms. *Biochim Biophys Acta*. 2014;1833(12):1-26. doi:10.1016/j.bbamcr.2013.06.028.ER.

16. Harding HP, Zhang Y, Ron D, Harding HP, Zhang Y, Ron D. Protein translation and folding are coupled by an endoplasmic reticulum-resident kinase. *Nature*. 1999;398(March):271-274.

17. Harding HP, Zhang Y, Bertolotti A, Zeng H, Ron D. Perk Is Essential for Translational Regulation and Cell Survival during the Unfolded Protein Response. *Mol Cell*. 2000;5:897-904.

18. Harding HP, Novoa I, Zhang Y, et al. Regulated Translation Initiation Controls Stress-Induced Gene Expression in Mammalian Cells. *Mol Cell*. 2000;6:1099-1108.

19. Zinszner H, Kuroda M, Wang X, et al. CHOP is implicated in programmed cell death in response to impaired function of the endoplasmic reticulum. *Genes Dev*. 1998;12:982-995.

20. Wang X, Kuroda M, Sok J, et al. Identification of novel stress-induced genes downstream of chop. *EMBO J*. 1998;17(13):3619-3630.

21. Cullough KDMC, Martindale JL, Klotz L, Aw T, Holbrook NJ. Gadd153 Sensitizes Cells to Endoplasmic Reticulum Stress by Down-Regulating Bcl2 and Perturbing the Cellular Redox State. *Mol Cell Biol*. 2001;21(4):1249-1259. doi:10.1128/MCB.21.4.1249.

22. Tirasophon W, Welihinda AA, Kaufman RJ. A stress response pathway from the endoplasmic reticulum to the nucleus requires a novel bifunctional protein kinase / endoribonuclease (Ire1p) in mammalian cells. *Genes Dev*. 1998;12:1812-1824.

23. Shamu CE, Walter P. Oligomerization and phosphorylation of the Irelp kinase during intracellular signaling from the endoplasmic reticulum to the nucleus. *EMBO J*. 1996;15(12):3028-3039.

24. Yoshida H, Matsui T, Yamamoto A, Okada T, Mori K. XBP1 mRNA Is Induced by ATF6 and Spliced by IRE1 in Response to ER Stress to Produce a Highly Active Transcription Factor. *Cell*. 2001;107:881-891.

25. Orr HA, Coyne JA, Mackay TFC, et al. Decay of Endoplasmic Reticulum-Localized mRNAs During the Unfolded Protein Response. *Science (80-)*. 2006;313(July):104-108.

26. Han D, Lerner AG, Walle L Vande, et al. IRE1α Kinase Activation Modes Control Alternate Endoribonuclease Outputs to Determine Divergent Cell Fates. *Cell*. 2010;138(3):562-575. doi:10.1016/j.cell.2009.07.017.IRE1.

27. Urano F, Wang X, Bertolotti A, et al. Coupling of Stress in the ER to Activation of JNK Protein Kinases by Transmembrane Protein Kinase IRE1. *Science (80-)*. 2000;287(January):664-667.

28. Andersen TB, López CQ, Manczak T, Martinez K, Simonsen HT. Thapsigargin-From Thapsia L. to Mipsagargin. *Molecules*. 2015;20(4):6113-6127.

doi:10.3390/molecules20046113.

29. Lytton J, Westlin M, Hanley MR. Thapsigargin inhibits the sarcoplasmic or endoplasmic reticulum Ca-ATPase family of calcium pumps. *J Biol Chem*. 1991;266(26):17067-17071. doi:VL - 266.

30. Doan NTQ, Paulsen ES, Sehgal P, et al. Targeting thapsigargin towards tumors. *Steroids*. 2015;97:2-7. doi:10.1016/j.steroids.2014.07.009.

31. Periasamy M, Kalyanasundaram A. SERCA pump isoforms: Their role in calcium transport and disease. *Muscle and Nerve*. 2007;35(4):430-442. doi:10.1002/mus.20745.

32. Dubois C, Vanden Abeele F, Sehgal P, et al. Differential effects of thapsigargin analogues on apoptosis of prostate cancer cells: complex regulation by intracellular calcium. *Febs J*. 2013;280(21):5430-5440. doi:10.1111/febs.12475.

33. Sehgal P, Szalai P, Olesen C, et al. Inhibition of the sarco/endoplasmic reticulum (ER) Ca2+-ATPase by thapsigargin analogs induces cell death via ER Ca2+ depletion and the unfolded protein response. *J Biol Chem*. 2017:jbc.M117.796920. doi:10.1074/jbc.M117.796920.

34. Denmeade SR, Jakobsen CM, Janssen S, et al. Prodrug as Targeted Therapy for Prostate Cancer. *J Natl Cancer Inst*. 2018;95(13).

35. Brennen WN, Rosen DM, Wang H, Isaacs JT, Denmeade SR. Targeting Carcinoma-Associated Fibroblasts Within the Tumor Stroma With a Fibroblast Activation Protein-Activated Prodrug. *J Nat Cancer Inst*. 2018;104(17):19-21. doi:10.1093/jnci/djs336.

36. Takatsuki, A., Arima, K., and Tamura G. Tunicamycin, a new antibiotic. I. Isolation and characterization of tunicamycin. *J Antibiot (Tokyo)*. 1970;XXIV(4).

37. Elbein AD. The tunicamycins- useful tools for studies on glycoproteins. *Trends Biochem Sci*. 1981;6:219-221.

38. Andresen L, Skovbakke SL, Persson G, Hagemann-jensen M, Hansen KA. 2-Deoxy d-Glucose Prevents Cell Surface Expression of NKG2D Ligands through Inhibition of N -Linked Glycosylation. *J Immunol*. 2012;188:1847-1855. doi:10.4049/jimmunol.1004085.

39. Schönthal AH. Endoplasmic Reticulum Stress: Its Role in Disease and Novel Prospects for Therapy. *Scientifica (Cairo)*. 2012;2012:1-26. doi:10.6064/2012/857516.

40. Klausner RD, Donaldson JG, Lippincott-Schwartz J. Brefeldin A: Insights into the Control of Membrane Traffic and Organelle Structure. *J Cell Biol*. 1992;116(5):1071-1080.

41. Yadav RK, Chae S, Kim H, Chae HJ. Endoplasmic Reticulum Stress and Cancer. *J Cancer Prev*. 2014;19(2):75-88.

42. Tsai YC, Weissman AM. The Unfolded Protein Response, Degradation from the Endoplasmic Reticulum, and Cancer. *Genes Cancer*. 2010;1(7):764-778. doi:10.1177/1947601910383011.

43. Healy SJM, Gorman AM, Mousavi-shafaei P, Gupta S, Samali A. Targeting the endoplasmic reticulum-stress response as an anticancer strategy. *Eur J Pharmacol*. 2009;625(1-3):234-246. doi:10.1016/j.ejphar.2009.06.064.

44. Patricia M, Sana O, Lisa K, Frank CR. Overexpression of the glucose-regulated stress gene GRP78 in malignant but not benign human breast lesions. *Breast Cancer Res Treat*. 2000;59:15-26.

45. Niu Z, Wang M, Zhou L, Yao L, Liao Q, Zhao Y. Elevated GRP78 expression is associated with poor prognosis in patients with pancreatic cancer. *Nat Publ Gr*. 2015;5(16067):1-12. doi:10.1038/srep16067.

46. Mhaidat NM, Alzoubi KH, Almomani N, Khabour OF. Expression of glucose regulated protein 78 (GRP78) determines colorectal cancer response to chemotherapy. *Cancer Biomarkers*. 2015;15:203-209. doi:10.3233/CBM-140454.

47. Wang YAN, Wang JH, Zhang XUNLEI, Wang XLI, Yang LEI. Endoplasmic reticulum chaperone glucose - regulated protein 78 in gastric cancer: An emerging biomarker. *Oncol Lett*. 2018;15:6087-6093. doi:10.3892/ol.2018.8114.

48. Fu W, Wu X, Li J, et al. Upregulation of GRP78 in Renal Cell Carcinoma and Its Significance. *J Urol*. 2010;75(3):603-607. doi:10.1016/j.urology.2009.05.007.

49. Lee HK, Xiang C, Cazacu S, et al. GRP78 is overexpressed in glioblastomas and regulates glioma cell growth and apoptosis. *Neuro Oncol*. 2008:236-243. doi:10.1215/15228517-2008-006.

50. Delie F, Petignat P, Cohen M. GRP78 protein expression in ovarian cancer patients and perspectives for a drug-targeting approach. *J Oncol*. 2012;2012:5. doi:10.1155/2012/468615.

51. Dong D, Ni M, Li J, et al. Critical role of the stress chaperone GRP78/BiP in tumor proliferation, survival, and tumor angiogenesis in transgene-induced mammary tumor development. *Cancer Res*. 2008;68(2):498-505. doi:10.1158/0008-5472.CAN-07-2950.

52. Urra H, Dufey E, Avril T, Chevet E, Hetz C. Endoplasmic Reticulum Stress and the Hallmarks of Cancer. *TRENDS in CANCER*. 2016;2(5):252-262. doi:10.1016/j.trecan.2016.03.007.

53. Schewe DM, Aguirre-ghiso JA. ATF6a-Rheb-mTOR signaling promotes survival of dormant tumor cells in vivo. *PNAS*. 2008;105(30):10519-10524.

54. Hanaoka M, Ishikawa T, Ishiguro M, Tokura M. Expression of ATF6 as a marker of pre-cancerous atypical change in ulcerative colitis-associated colorectal cancer: a potential role in the management of dysplasia. *J Gastroenterol*. 2018;53(5):631-641. doi:10.1007/s00535-017-1387-1.

55. Dadey DYA, Kapoor V, Khudanyan A, et al. The ATF6 pathway of the ER stress response contributes to enhanced viability in glioblastoma. *Oncotarget*. 2015;7(2):2080-2092.

56. Wang, Y., Alam, G.N., Ning, Y., Visioli, F., Dong, Z., Nör, J.E., and Polverini PJ. The Unfolded Protein Response Induces the Angiogenic Switch in Human Tumor Cells

through the PERK/ATF4 Pathway Yugang. *Cancer Res*. 2013;72(20):5396-5406. doi:10.1158/0008-5472.CAN-12-0474.The.

57. Notte A, Rebucci M, Fransolet M, et al. Taxol-induced unfolded protein response activation in breast cancer cells exposed to hypoxia: ATF4 activation regulates autophagy and inhibits apoptosis. *Int J Biochem Cell Biol*. 2015;62:1-14. doi:10.1016/j.biocel.2015.02.010.

58. Kouroku Y, Fujita E, Tanida I, et al. ER stress (PERK/eIF2 a phosphorylation) mediates the polyglutamine-induced LC3 conversion, an essential step for autophagy formation. *Cell Death Differ*. 2007;1:230-239. doi:10.1038/sj.cdd.4401984.

59. Mujcic H, Nagelkerke A, Rouschop KMA, et al. Hypoxic Activation of the PERK/eIF2a Arm of the Unfolded Protein Response Promotes Metastasis through Induction of LAMP3. *Hum Cancer Biol*. 2013;19(8):6126-6138. doi:10.1158/1078-0432.CCR-13-0526.

60. DeZwaan-McCabe D, Riordan JD, Arensdorf AM, Icardi MS, Dupuy AJ, Rutkowski DT. The Stress-Regulated Transcription Factor CHOP Promotes Hepatic Inflammatory Gene Expression, Fibrosis, and Oncogenesis. *PLoS Genet*. 2013;9(12). doi:10.1371/journal.pgen.1003937.

61. Fujimoto T, Onda M, Nagai H, Nagahata T, Ogawa K, Emi M. Upregulation and overexpression of human X-box binding protein 1 (hXBP-1) gene in primary breast cancers. *Breast Cancer*. 2003;10(4):301-306. http://www.ncbi.nlm.nih.gov/pubmed/14634507.

62. Koong AC, Chauhan V, Romero-Ramirez L. Targeting XBP-1 as a novel anti-cancer strategy. *Cancer Biol Ther*. 2006;5(7):756-759. doi:10.4161/cbt.5.7.2973.

63. Shuda M. KNYM et al. Activation of the ATF6, XBP1 and grp78 genes in human hepatocellular carcinoma: a possible involvement of the ER stress pathway in hepatocarcinogenesis. *J Hepatol*. 2003;38:605-614. doi:10.1016/S0.

64. Chen X, Iliopoulos D, Zhang Q, et al. XBP1 promotes triple-negative breast cancer by controlling the HIF1α pathway. *Nature*. 2014;508(1):103-107. doi:10.1038/nature13119.

65. Mimura N, Fulciniti M, Gorgun G, et al. Blockade of XBP1 splicing by inhibition of IRE1a is a promising therapeutic option in multiple myeloma. *Blood*. 2012;119(24):5772-5782. doi:10.1182/blood-2011-07-366633.The.

66. Thorpe JA, Schwarze SR. IRE1α controls cyclin A1 expression and promotes cell proliferation through XBP-1. *Cell Stress Chaperones*. 2010;15(5):497-508. doi:10.1007/s12192-009-0163-4.

67. Li XX, Zhang HS, Xu YM, et al. Knockdown of IRE1α inhibits colonic tumorigenesis through decreasing α-catenin and IRE1α targeting suppresses colon cancer cells. *Oncogene*. 2017;36(48):6738-6746. doi:10.1038/onc.2017.284.

68. Cubillos-Ruiz JR, Glimcher LH. Targeting abnormal ER stress responses in tumors: A new approach to cancer immunotherapy. *Oncoimmunology*. 2016;5(3):1-3. doi:10.1080/2162402X.2015.1098802.

69. Rappa F, Farina F, Zummo G, et al. HSP-Molecular chaperones in cancer biogenesis and tumor therapy: An overview. *Anticancer Res*. 2012;32(12):5139-5150.

70. Crowley VM, Huard DJE, Lieberman RL, Blagg BSJ. Second Generation Grp94-Selective Inhibitors Provide Opportunities for the Inhibition of Metastatic Cancer. *Chem - A Eur J*. 2017;23(62):15775-15782. doi:10.1002/chem.201703398.

71. Hua Y, White-gilbertson S, Kellner J, Rachidi S, Usmani SZ. Molecular Chaperone gp96 Is a Novel Therapeutic Target of Multiple Myeloma. *Clin Cancer Res*. 2013;19(22):6242-6252. doi:10.1158/1078-0432.CCR-13-2083.

72. Kerr JFR, Wyllie AH CA. Apoptosis: A Basic Biological Phenomenon With Wide-Ranging Implications in Tissue Kinetics. *Br J Cancer*. 1972;26:239-257.

73. Elmore S. Apoptosis: a review of programmed cell death. *Toxicol Pathol*. 2007;35(4):495-516. doi:10.1080/01926230701320337.

74. Horvitz R, Yuan J. The Caenorhabditis elegans Genes ced-3 and ced-4 Act Cell Autonomously to Cause Programmed Cell Death. *Dev Biol*. 1990;41:33-41.

75. Mcilwain DR, Berger T, Mak TW. Caspase Functions in Cell Death and Disease. *Cold Spring Harb Perspect Biol*. 2013;5:5:a008656. doi:10.1101/cshperspect.a008656.

76. Suzanne M, Steller H. Shaping organisms with apoptosis. *Cell Death Differ*. 2013;20(5):669-675. doi:10.1038/cdd.2013.11.

77. Schultz DR, Harrington WJ. Apoptosis: Programmed Cell Death at a Molecular Level. *Semin Arthritis Rheum*. 2003;32(6):345-369. doi:10.1053/sarh.2003.50005.

78. Kroemer G, Galluzzi L, Brenner C. Mitochondrial Membrane Permeabilization in Cell Death. *Physiol Rev*. 2007;87:99-163. doi:10.1152/physrev.00013.2006.

79. Li H, Zhu H, Xu C, Yuan J. Cleavage of BID by Caspase 8 Mediates the Mitochondrial Damage in the Fas Pathway of Apoptosis. *Cell*. 1998;94:491-501.

80. Shamas-din A, Kale J, Leber B, Andrews DW. Mechanisms of Action of Bcl-2 Family Proteins. *Cold Spring Harb Perspect Biol*. 2013;(5):1-21. doi:10.1101/cshperspect.a008714.

81. Bhola PD, Letai A. Mitochondria-Judges and Executioners of Cell Death Sentences. *Mol Cell*. 2016;61(5):695-704. doi:10.1016/j.molcel.2016.02.019.

82. Happo L, Strasser A. BH3-only proteins in apoptosis at a glance. *J Cell Sci*. 2012;125:1081-1087. doi:10.1242/jcs.090514.

83. Czabotar PE, Lessene G, Strasser A, Adams JM. Control of apoptosis by the BCL-2 protein family: implications for physiology and therapy. *Nat Rev Mol Cell Biol*. 2014;15(1):49-63. doi:10.1038/nrm3722.

84. Wei MC, Zong W, Cheng EH, et al. Proapoptotic BAX and BAK: A Requisite Gateway to Mitochondrial Dysfunction and Death. *Science (80-)*. 2011;292(5517):727-730. doi:10.1126/science.1059108.Proapoptotic.

85. Scorrano L, Oakes SA, Opferman JT, et al. BAX and BAK Regulation of Endoplasmic Reticulum Calcium: A Control Point for Apoptosis. *Science (80-)*. 2003;300(April):135-140.

86. Iurlaro R. Cell death induced by endoplasmic reticulum stress. *FEBS J*. 2016;283:2640-2652. doi:10.1111/febs.13598.

87. Li J, Lee B, Lee AS. Endoplasmic reticulum stress -induced apoptosis: multiple pathways and activation of p53 -up-regulated modulator of apoptosis (PUMA) and NOXA by p53. *J Biol Chem*. 2006;281(11):7260-7270. doi:10.1074/jbc.M509868200.

88. Logue SE, Cleary P, Saveljeva S, Samali A. New directions in ER stress-induced cell death. *Apoptosis*. 2013;18(5):537-546. doi:10.1007/s10495-013-0818-6.

89. Puthalakath H, Reilly LAO, Gunn P, et al. ER Stress Triggers Apoptosis by Activating BH3-Only Protein Bim. *Cell*. 2007;129:1337-1349. doi:10.1016/j.cell.2007.04.027.

90. Yip KW, Reed JC. Bcl-2 family proteins and cancer. *Oncogene*. 2008;27:6398-6406. doi:10.1038/onc.2008.307.

91. Lagares-tena L, Mjiyad N El, Ramírez-peinado S, Alc F. 2-Deoxyglucose Induces Noxa-Dependent Apoptosis in Alveolar Rhabdomyosarcoma. *Cancer Res*. 2011;71(21):6796-6807. doi:10.1158/0008-5472.CAN-11-0759.

92. Yamaguchi H, Wang H. CHOP Is Involved in Endoplasmic Reticulum Stress-induced Apoptosis by Enhancing DR5 Expression in Human Carcinoma Cells. *J Biol Chem*. 2004;279(44):45495-45502. doi:10.1074/jbc.M406933200.

93. Gomez BP, Riggins RB, Shajahan AN, et al. Human X-Box binding protein-1 confers both estrogen independence and antiestrogen resistance in breast cancer cell lines. *FASEB J*. 2007:4013-4027. doi:10.1096/fj.06-7990com.

94. Szegezdi E, Macdonald DC. Bcl-2 family on guard at the ER. *J Physiol Cell Physiol*. 2009;296:941-953. doi:10.1152/ajpcell.00612.2008.

95. White C, Li C, Yang J, et al. The endoplasmic reticulum gateway to apoptosis by Bcl-XL modulation of the InsP3R. *Nat Cell Biol*. 2005;7(10). doi:10.1038/ncb1302.

96. Li G, Mongillo M, Chin K, et al. Role of ERO1-alpha–mediated stimulation of inositol 1,4,5-triphosphate receptor activity in endoplasmic reticulum stress–induced apoptosis. *J Cancer Prev*. 2009;186(6):783-792. doi:10.1083/jcb.200904060.

97. Chernorudskiy AL, Zito E. Regulation of Calcium Homeostasis by ER Redox: A Close-Up of the ER/Mitochondria Connection. *J Mol Biol*. 2017;429(5):620-632. doi:10.1016/j.jmb.2017.01.017.

98. Zecchini E, Pinton P. Ca2+ transfer from the ER to mitochondria: when, how and why. *Biochim Biophys Acta*. 2010;1787(11):1342-1351. doi:10.1016/j.bbabio.2009.03.015.

99. Szado T, Vanderheyden V, Parys JB, et al. Phosphorylation of inositol 1,4,5-trisphosphate receptors by protein kinase B/Akt inhibits Ca 2+ release and apoptosis. *PNAS*. 2008;105(7):2427-2432.

100. Smith TM, Hicks-berger CA, Kim S, Kirley TL. Cloning, expression, and characterization of a soluble calcium-activated nucleotidase, a human enzyme belonging to a new family of extracellular nucleotidases. *Arch Biochem Biophys*. 2002;406:105-115.

101. Murphy DM, Ivanenkov V V, Kirley TL. Bacterial Expression and Characterization

of a Novel, Soluble, Calcium-Binding, and Calcium-Activated Human Nucleotidase. *Biochemistry*. 2003;42:2412-2421. doi:10.1021/bi026763b.

102. Yang M, Kirley TL. Site-Directed Mutagenesis of Human Soluble Calcium-Activated Nucleotidase 1 (hSCAN-1): Identification of Residues Essential for Enzyme Activity and the Ca2+-Induced Conformational Change. *Biochemistry*. 2004;1:9185-9194.

103. Failer BU, Braun N, Zimmermann H. Cloning, Expression, and Functional Characterization of a Ca2+-dependent Endoplasmic Reticulum Nucleoside Diphosphatase. *J Biol Chem*. 2002;277(40):36978-36986. doi:10.1074/jbc.M201656200.

104. Faden M, Al-zahrani F, Arafah D, Alkuraya FS. Mutation of CANT1 Causes Desbuquois Dysplasia. *Am J Med Genet*. 2010;152(April):1157-1160. doi:10.1002/ajmg.a.33404.

105. Bertoli M, Chami M, Alanay Y, et al. Identification of CANT1 Mutations in Desbuquois Dysplasia. *Am J Hum Genet*. 2009;85:706-710. doi:10.1016/j.ajhg.2009.10.001.

106. Kim O, Nishimura G, Song H, et al. A Variant of Desbuquois Dysplasia Characterized by Advanced Carpal Bone Age, Short Metacarpals, and Elongated Phalanges: Report of Seven Cases. *Am J Med Genet*. 2010;(March):875-885. doi:10.1002/ajmg.a.33347.

107. Nizon M, Leonardis F De, Merrina R, et al. Further Delineation of CANT1 Phenotypic Spectrum and Demonstration of Its Role in Proteoglycan Synthesis. *Hum Mutat*. 2012;33(8):1261-1266. doi:10.1002/humu.22104.

108. Balasubramanian K, Li B, Krakow D, et al. MED resulting from recessively inherited mutations in the gene encoding calcium-activated nucleotidase CANT1. 2017;(May):2415-2421. doi:10.1002/ajmg.a.38349.

109. Hermans KG, Bressers AA, Korput HA Van Der, Dits NF, Jenster G, Trapman J. Two Unique Novel Prostate-Specific and Androgen-Regulated Fusion Partners of ETV4 in Prostate Cancer. *Cancer Res*. 2008;68(9):3094-3099. doi:10.1158/0008-5472.CAN-08-0198.

110. Gerhardt J, Steinbrech C, Büchi O, et al. The Androgen-Regulated Calcium-Activated Nucleotidase 1 (CANT1) Is Commonly Overexpressed in Prostate Cancer and Is Tumor-Biologically Relevant in Vitro. *AJPA*. 2011;178(4):1847-1860. doi:10.1016/j.ajpath.2010.12.046.

111. Calì T, Fedrizzi L, Ottolini D, et al. Ca2+ -activated Nucleotidase 1, a Novel Target Gene for the Transcriptional Repressor DREAM (Downstream Regulatory Element Antagonist Modulator), Is Involved in Protein Folding and Degradation. *J Biol Chem*. 2012;287(22):18478-18491. doi:10.1074/jbc.M111.304733.

112. Uccelletti D, Pascoli A, Farina F, et al. APY-1, a Novel Caenorhabditis elegans Apyrase Involved in Unfolded Protein Response Signalling and Stress Responses. *Mol Biol Cell*. 2008;19(April):1337-1345. doi:10.1091/mbc.E07.

113. Livak KJ, Schmittgen TD. Analysis of relative gene expression data using real-time quantitative PCR and the 2-ΔΔCT method. *Methods*. 2001;25(4):402-408.

doi:10.1006/meth.2001.1262.

114. Zinchuk V, Zinchuk O. Quantitative Colocalization Analysis of Confocal Fluorescence Microscopy Images. *Curr Protoc Cell Biol*. 2008;(June):1-16. doi:10.1002/0471143030.cb0419s39.

115. Neve RM, Chin K, Fridlyand J, et al. A collection of breast cancer cell lines for the study of functionally distinct cancer subtypes. *Cancer Cell*. 2006;10(December):515-527. doi:10.1016/j.ccr.2006.10.008.

116. Holliday DL, Speirs V. Choosing the right cell line for breast cancer research. *Breast Cancer Res*. 2011;13:215-221. doi:10.1186/bcr2889.

117. Xing L, Hung M, Bonfiglio T, Hicks DG, Tang P. Breast Cancer : Basic and Clinical Research The Expression Patterns of ER, PR, HER2, CK5/6, EGFR, Ki-67 and AR by Immunohistochemical Analysis in Breast Cancer Cell Lines. *Breast Cancer Basic Clin Res*. 2010;4(35-41):35-41.

118. Mazumdar A, Poage GM, Shepherd J, et al. Analysis of phosphatases in ER-negative breast cancers identifies DUSP4 as a critical regulator of growth and invasion. *Breast Cancer Res Treat*. 2016;158(3):441-454. doi:10.1007/s10549-016-3892-y.

119. Jackisch C, Hahm HA, Tombal B, et al. Delayed Micromolar Elevation in Intracellular Calcium Precedes Induction of Apoptosis in Thapsigargin-treated Breast Cancer Cells. *Clin Cancer Res*. 2000;6(July):2844-2850.

APPENDIX A – Chemicals

Chemicals and Media Components	Supplier Company
Acrylamide/Bis-acrylamide	Sigma, Germany
APS	Amresco, USA
Bradford solution	Biorad, USA
BSA	Gemini, USA
Chaps	Sigma, Germany
DAPI	Life Technologies, USA
Distilled water	Milipore, France
DMSO	Sigma, Germany
DMSO	AppliChem, Germany
DMEM/F12	Thermo Fisher Scientific, UK
EDTA	Riedel-de Haen, Germany
EGTA	Riedel-de Haen, Germany
ER-Tracker Red	Life Technologies, USA
Ethanol	Merck, Germany
FBS	Pan, Fermany
Glycerol	Sigma, Germany
Glycine	Molekula, UK
HCl	Merck, Germany
Isopropanol	Merck, Germany
KCl	Amresco, USA
KH2PO4	Riedel-de Haen, Germany
Liquid nitrogen	Karbogaz, Turkey
Methanol	Sigma, Germany
$MgCl_2$	Sigma, Germany
Milk diluent concentrate	KPL, USA
Milk powder (non-fat, dried)	AppliChem, Germany

Mito-Tracker Red	Life Technologies, USA
Na2HPO4	Merck, Germany
NaCl	Merck, Germany
NaOH	Merck, Germany
Paraformaldehyde	Sigma, Germany
PBS	PAN, Germany
Penicillin-Streptomycin	Life Technologies, USA
phoSTOP phosphatase inhibitor	Roche, Germany
Protease inhibitor cocktail tablet	Roche, Germany
PVDF membrane	Roche, Germany
Sodium Dodecyl Sulphate	Sigma, Germany
TEMED	Sigma, Germany
Thapsigargin	Sigma, Germany
Tris	AppliChem, Germany
Trypan Blue	NanoEnTek, Korea
Trypsin-EDTA	PAN, Germany
TritonX-100	Sigma, Germany
Tween20	Sigma, Germany

APPENDIX B – Equipment

Equipment	Supplier Company
Autoclave	Hirayama, Hiclave HV-110, Japan
Balance	Sartorius, BP221S, Germany
Cell Counter	NanoEnTek, Korea
Centrifuge	Kendro Lab. Prod., Multifuge 3S-R, Heraeus, Germany
	Eppendorf, 5415D, Germany
	Eppendorf, 5424R, Germany
	Eppendorf, 5430R, Germany
	ScanSpeen Mini, Labogene, Denmark
CO_2 Incubator	Binder, Germany
Computer Software	CoLocalizer Pro 3.0.2
	GraphPad Prism 5
	ImageJ 1.51w
Deepfreeze	-80°C, Kendro Lab Prod., Heraeus Hfu486Basic, Germany
	-20°C, Bosch, Turkey
Distilled Water	Millipore, Elix-S, France
Gel Electrophoresis and Blotting System	Mini-PROTEAN Tetra Cell, Biorad, Mini-PROTEAN 3 Cell, Biorad, USA

Heat Block	Bio TDB-100, Biosan SIA, Latvia
Hemocytometer	Hausser Scientific,Blue Bell Pa.,USA
Ice Machine	Scotsman Inc., AF20, USA
Imaging System (Western Blot)	LAS4000 mini, Fujifilm, Japan
Laminar Flow	Kendro Lab. Prod., Heraeus, HeraSafe HS12, Germany
Liquid Nitrogen Tank	Taylor-Wharton, 3000RS, USA
Magnetic Stirrer	VELP Scientifica, ARE Heating Magnetic Stirrer, Italy
Microliter Pipettes	Gilson, Pipetman, France
	Eppendorf, Germany
Microscope	LSM 710, Confocal Laser Scanning Microscope, Zeiss, Germany
	Olympus CKX41, Japan
Microscope Slides	0.17mm, Thermo Fisher Scientific, USA
Microtiter Plate Reader	Microplate Reader 680, Biorad, USA
pH meter	WTW, pH540 GLP MultiCal, Germany
Power Supply	Biorad, PowerPac 300, USA
	Wealtec, Elite 300, USA
Refrigerator	Bosch, Turkey
Shaker-Rotater	Gyro-rocker SSL3, Stuart, UK
	IKA KS 260 Basic, USA
	Labquake, ThermoScientific, USA
Spectrophotometer	ND-1000, Nanodrop, USA
Thermocycler	LightCycler 480, Roche, Germany
Vortex	Velp Scientifica, Italy

Water Bath	Huber, Polystat cc1, Germany

APPENDIX C – Solutions and Buffers

0.1% Blocking solution (0.1% BSA)
0.1 g BSA
100 ml 1X PBS

0.5% Triton-X100 solution
250 µl TritonX-100
50 ml 1X PBS

1% Chaps buffer
500 µl 1M $MgCl_2$
13.7 ml 1M NaCl
1 ml 100 mM EDTA
1 ml 100 mM EGTA
1 g Chaps
0.242 g Tris
complete to 100 ml with dH_2O
add protease and phosphatase inhibitors

4% PFA
4 g Paraformaldehyde
70 g dH_2O
200 µl 5M NaOH
10 ml 10X PBS
complete to 100 ml with dH_2O

10% APS
0.1 g APS
1 ml dH_2O

Mounting medium
50% Glycerol in 1X PBS

PBS (10X)
80 g NaCl
2.25 g KCl
23.27 g $Na_2HPO_4.12H_2O$
2.05 g KH_2PO_4
complete to 1000 ml with dH_2O
adjust pH to 7.4

Running buffer
30.3 g Tris
144.1 g Glycine
10 g SDS
complete to 1000 ml with dH_2O
adjust pH to 8.3

Transfer buffer (10X-stock solution)
144.2 g Glycine
30.8 g Tris
complete to 1000 ml with dH_2O

Transfer buffer (1X-working solution)
70 ml 10X Transfer buffer
140 ml Methanol
490 ml dH_2O

Tris-HCl-SDS (pH:6.8)
6.05 g Tris
100 ml dH_2O
adjust pH to 6.8 with 1N HCl
add 0.4 g SDS

Tris-HCl-SDS (pH:8.8)
91 g Tris
500 ml dH_2O
adjust pH to 8.8 with 1 N HCl
add 2 g SDS

Western Blot blocking solution - 5% milk
5 g non-fat dried milk
100 ml washing solution

Western Blot washing solution - PBS-Tween20 (PBST) solution (1X)
100 ml PBS (10X)
900 ml dH_2O
2 ml Tween20

Western Blot primary antibody incubation solution
3200 µl dH_2O
4 µg antibody
400 µl milk diluent
400 µl PBS-T

Western Blot secondary antibody incubation solution
1 µg antibody
10 ml 5% milk

APPENDIX D – Molecular Biology Kits and Reagents

Commercial Kit	Supplier Company
Cell Proliferation Reagent WST-1	Roche, Germany
Luminata Crescendo Western HRP Substrate	Millipore, USA
RNeasy Mini Kit (74104)	Qiagen, Germany
QuantiTect SYBR Green RT-PCR Kit	Qiagen, Germany
QuantiTect Primer Assay Hs_CANT1_1_SG	Qiagen, Germany
QuantiTect Primer Assay Hs_GAPDH_1_SG	Qiagen, Germany

APPENDIX E – Antibodies

Antibody / Catalog Number	Supplier Company
Anti-CANT1 Monoclonal (C-3) /sc-515574	Santa Cruz Biotechnology
Anti-β-Actin Monoclonal / 4967L	Cell Signaling Technologies
Anti-Mouse HRP-conjugated / 7076	Cell Signaling Technologies
Anti-Rabbit HRP-conjugated / 7074	Cell Signaling Technologies
Alexa Fluor® 488 anti-mouse / A-11029	Thermo Fisher Scientific

APPENDIX F – ATCC Breast Cancer Cell Panel (30-4500K™)

Cell Line	ATCC Code
184B5	ATCC CRL-8799
AU-565	ATCC CRL-2351
BT-20	ATCC HTB-19
BT-474	ATCC HTB-20
BT-483	ATCC HTB-121
BT-549	ATCC HTB-122
CAMA-1	ATCC HTB-21
DU4475	ATCC HTB-123
HCC38	ATCC CRL-2314
HCC70	ATCC CRL-2315
HCC202	ATCC CRL-2316
HCC1187	ATCC CRL-2322
HCC1395	ATCC CRL-2324
HCC1419	ATCC CRL-2326
HCC1428	ATCC CRL-2327
HCC1500	ATCC CRL-2329
HCC1569	ATCC CRL-2330
HCC1599	ATCC CRL-2331
HCC1806	ATCC CRL-2335
HCC1937	ATCC CRL-2336
HCC1954	ATCC CRL-2338
HCC2157	ATCC CRL-2340
HCC2218	ATCC CRL-2343
Hs 578Bst	ATCC HTB-125
Hs 578T	ATCC HTB-126
MCF7	ATCC HTB-22
MCF 10A	ATCC CRL-10317
MCF 10F	ATCC CRL-10318
MCF-12A	ATCC CRL-10782
MDA-kb2	ATCC CRL-2713
MDA-MB-134-6	ATCC HTB-23
MDA-MB-157	ATCC HTB-24
MDA-MB-175-7	ATCC HTB-25
MDA-MB-231	ATCC HTB-26
MDA-MB-361	ATCC HTB-27
MDA-MB-415	ATCC HTB-128
MDA-MB-436	ATCC HTB-130
MDA-MB-453	ATCC HTB-131
MDA-MB-468	ATCC HTB-132
SK-BR-3	ATCC HTB-30
T47D	ATCC HTB-133
UACC-812	ATCC CRL-1897
UACC-893	ATCC CRL-1902
ZR-75-1	ATCC CRL-1500
ZR-75-30	ATCC CRL-1504

APPENDIX G – Protein Molecular Weight Marker

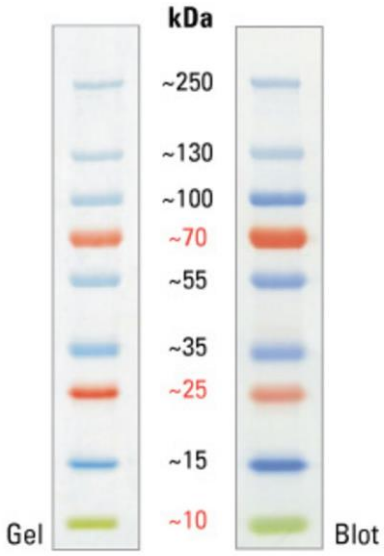

Figure G.1. PageRuler™ Plus Prestained Protein Ladder (#26619), Thermo Scientific